PB81-179848

Atmospheric Measurements of Trace Pollutants Long Path Fourier Transform Infrared Spectroscopy

California Univ., Riverside

Prepared for

Environmental Sciences Research Lab
Research Triangle Park, NC

Apr 81

U.S. Department of Commerce
National Technical Information Service
NTIS.

TECHNICAL REPORT DATA
(Please read Instructions on the reverse before completing)

1. REPORT NO. EPA-600/3-81-026	2.
3. REC PB81-179848	
4. TITLE AND SUBTITLE ATMOSPHERIC MEASUREMENTS OF TRACE POLLUTANTS Long Path Fourier Transform Infrared Spectroscopy	5. REPORT DATE April 1981 6. PERFORMING ORGANIZATION CODE
7. AUTHOR(S) Tuazon, E.C., A.M. Winer, R.A. Graham, and J.N. Pitts, Jr.	8. PERFORMING ORGANIZATION REPORT NO.
9. PERFORMING ORGANIZATION NAME AND ADDRESS Statewide Air Pollution Research Center University of California Riverside, California 92521	10. PROGRAM ELEMENT NO. CDWA1A/01 - 0641 (FY-81) 11. CONTRACT/GRANT NO. R-804546
12. SPONSORING AGENCY NAME AND ADDRESS Environmental Sciences Research Laboratory-RTP, NC Office of Research and Development U.S. Environmental Protection Agency Research Triangle Park, North Carolina 27711	13. TYPE OF REPORT AND PERIOD COVERED Final 6/76 - 5/80 14. SPONSORING AGENCY CODE EPA/600/09
15. SUPPLEMENTARY NOTES	

16. ABSTRACT

Described are the results of a four-year study to measure trace pollutant concentrations in polluted atmospheres by kilometer pathlength Fourier transform infrared (FT-IR) absorption spectroscopy. The study covers selected smog episodes during the years 1976 to 1979. During 1976 and 1977 the FT-IR facility was operated in Riverside, CA, and recorded spectra from smog episodes which provided valuable benchmark data. In 1978 and 1979 the FT-IR facility was operated in Claremont, CA, a location chosen to characterize episodes closer to the Pasadena-Azusa area which experiences the highest smog levels. During 1978 the study focussed on extended monitoring periods and succeeded in recording a "classic" stagnant air episode with pollutant "carryover" and progressively increasing oxidant levels. Research in 1979 consisted of collaborative studies to validate newly developed analytical and sampling techniques for measuring HNO_3, NH_3, and HCHO. In these studies the km pathlength FT-IR spectroscopic technique served as the reference method. The ambient air data collected for trace pollutant concentrations over the four-year period, together with the results of several collaborative studies to validate new methods, will provide a critically needed data base for stringently testing the chemical kinetic submodels of the current generation of widely used urban airshed models.

17. KEY WORDS AND DOCUMENT ANALYSIS

a. DESCRIPTORS	b. IDENTIFIERS/OPEN ENDED TERMS	c. COSATI Field/Group

18. DISTRIBUTION STATEMENT RELEASE TO PUBLIC	19. SECURITY CLASS *(This Report)* UNCLASSIFIED 20. SECURITY CLASS *(This page)* UNCLASSIFIED	21. NO. OF PAGES 104 22. PRICE

EPA Form 2220-1 (Rev. 4-77) PREVIOUS EDITION IS OBSOLETE

PRODUCT OF:
NATIONAL TECHNICAL
INFORMATION SERVICE
U.S. DEPARTMENT OF COMMERCE
SPRINGFIELD, VA. 22161

EPA 600/3-81-026
April 1981

ATMOSPHERIC MEASUREMENTS OF TRACE POLLUTANTS
Long Path Fourier Transform Infrared Spectroscopy

by

Ernesto C. Tuazon, Arthur M. Winer, Richard A. Graham,
and James N. Pitts, Jr.
Statewide Air Pollution Research Center
University of California
Riverside, CA 92521

EPA Grant Number R-804546

Project Officers

Philip L. Hanst
Bruce W. Gay, Jr.
John W. Spence

Atmospheric Chemistry and Physics Division
Environmental Sciences Research Laboratory
Research Triangle Park, NC 27711

ENVIRONMENTAL SCIENCES RESEARCH LABORATORY
OFFICE OF RESEARCH AND DEVELOPMENT
U.S. ENVIRONMENTAL PROTECTION AGENCY
RESEARCH TRIANGLE PARK, NC 27711

DISCLAIMER

This report has been reviewed by the Environmental Sciences Research Laboratory, U.S. Environmental Protection Agency, and approved for publication. Approval does not signify that the contents necessarily reflect the view and policies of the U.S. Environmental Protection Agency, nor does mention of trade names or commercial products constitute endorsement or recommendation for use.

ABSTRACT

This report describes the results of a four-year study to measure trace pollutant concentrations in polluted atmospheres by kilometer path-length Fourier transform infrared (FT-IR) absorption spectroscopy. The study was conducted at two sites in the California South Coast Air Basin (CSCAB) and covered selected smog episodes which occcurred during the years 1976 to 1979.

During 1976 and 1977 the FT-IR facility was operated in Riverside, California, a location approximately 60 miles east, and 8-12 hours downwind, of the primary emission sources in the Los Angeles area. Due to unusual meteorological conditions which resulted in a low incidence of pollution episodes, our first year monitoring efforts succeeded in recording data from only three moderate smog episodes which occurred in October, 1976. Nevertheless, these measurements provide valuable benchmark data, including the first reported direct spectroscopic detection of trace levels of nitric acid (HNO_3) and formaldehyde (HCHO) in the polluted troposphere.

A larger number of smog episodes were experienced in Riverside during the following year (1977), and the results from 5 to 8 hour monitoring periods for 10 selected episode days are contained in this report. These measurements verify the suspected prevalence of high ammonia (NH_3) concentrations (>100 ppb in some instances) in the Riverside area which originate primarily from surrounding agricultural sources. Analysis of the simultaneous concentration data for HNO_3 and NH_3 led to the conclusion that the ammonium nitrate equilibrium constant derived from published thermochemical data gives a reasonable upper limit for the concentration product of gas-phase HNO_3 and NH_3 in a polluted atmosphere.

The second year of the program (1977) also included the measurements of accurate absorptivity values for the pollutant species of interest in this study. This resulted in the correction of discrepancies, particularly serious in the case of formic acid (HCOOH), brought about by our initial use of literature values which were based on measurements at lower spectral resolutions. Thus, this report contains a re-analysis of the previously published 1976 Riverside data, based on our more recent absorptivity measurements.

During the last two years of the study (1978 and 1979), the FT-IR facility was operated in Claremont, California, a mid-basin site between Riverside and the Los Angeles metropolitan area. This location allowed us to characterize episodes closer to the locations experiencing the highest

smog levels (Pasadena-Azusa area) in the CSCAB. Claremont is also more typical than Riverside of other locations in the CSCAB in terms of generally low concentrations of NH_3 ($\leq$10 ppb).

The 1978 study focused on extended monitoring periods and succeeded in recording a "classic" stagnant air episode with pollutant "carryover" and progressively increasing oxidant levels during the week of October 9-13, 1978. The FT-IR measurements included a 38-hour continuous monitoring period for the more severe episodes of October 12 and 13, 1978. The most intense episode of that week (October 13) was characterized by peak pollutant levels of 454 ppb O_3, 37 ppb PAN, 49 ppb HNO_3, 19 ppb HCOOH, and 71 ppb HCHO.

Our fourth year efforts (1979) consisted of collaborative studies with workers from other research organizations to validate newly developed analytical and sampling techniques for measuring HNO_3, NH_3, and HCHO. In these studies the km pathlength FT-IR spectroscopic technique served as the reference method. Among the studies conducted was a major EPA-sponsored field study program to intercompare current analytical methods for gaseous HNO_3 and particulate nitrate. A partial analysis of the HNO_3 measurement data, which were obtained at the location of our FT-IR facility in Claremont during the period August 27-September 3, 1979, is presented in this report.

We believe that the ambient air data which we have obtained for trace pollutant concentrations over a four-year period (based in a number of cases on remeasured absorptivities), together with the results of our several collaborative studies to validate new methods of analysis of "non-criteria" pollutants, will provide a critically needed data base for stringently testing the chemical kinetic submodels of the current generation of widely used urban airshed models.

This report was submitted in fulfillment of grant R-804546 by the University of California Statewide Air Pollution Research Center, Riverside, California, 92521, under the sponsorship of the U.S. Environmental Protection Agency. This report covers a period from June 1976 to May 1980 and work was completed as of May 1980.

CONTENTS

Abstract iii

Figures vi

Tables viii

Acknowledgements ix

1. Introduction 1

2. Background 5

3. Instrumentation and Methods 7

   A. Description of the Fourier transform infrared spectrometer and kilometer pathlength cell 7

   B. Operation of the long-path FT-IR system 10

   C. Spectral processing 11

   D. Detailed considerations pertaining to optimum instrument performance and accuracy of spectral data 11

   E. FT-IR absorptivities and detection limits 14

4. Measurement of Pollutants in Ambient Air 18

   A. First year of study 18

   B. Second year of study 26

   C. Third year of study 31

   D. Fourth year of study 40

   E. Attempts to detect other species 50

5. Conclusions 56

6. Recommended Improvements in Instrumentation 58

References 63

Appendix A

Ambient Air Measurements 70

FIGURES

Number		Page
1	Eight mirror multiple reflection system.	8
2	Kilometer pathlength FT-IR system.	9
3	Riverside ambient air spectra at 0.5 cm^{-1} spectral resolution, 1080 m pathlength. NH_3 concentration, 44 ppb. .	20
4	Riverside ambient air spectra at 0.5 cm^{-1} spectral resolution, 1080 m pathlength. Formaldehyde concentration, 11 ppb.	21
5	Riverside ambient air spectrum (October 5, 1976 at 7:22 p.m.) at 0.5 cm^{-1} spectral resolution, 1080 m pathlength. Nitric acid concentration, 8 ppb	22
6	Reference spectra at 0.5 cm^{-1} spectral resolution and 1080 m pathlength: (a) ammonia, ~200 ppb; (b) formaldehyde, ~270 ppb; (c) nitric acid, ~150 ppb.	23
7	Riverside ambient air spectrum (October 5, 1976 at 6:33 p.m.) at 0.5 cm^{-1} spectral resolution, 1080 m pathlength. Formic acid, 7 ppb; ozone, 205 ppb	24
8	Comparison of FT-IR and UV analyzer measurements of ambient ozone concentrations	25
9	Riverside ambient air spectra at 0.5 cm^{-1} spectral resolution and 900 m pathlength with InSb detector.	27
10	Riverside ambient air spectrum (August 12, 1977 at 12:32 p.m.) at 0.5 cm^{-1} spectral resolution and 900 m pathlength with HgCdTe detector.	28
11	Time-concentration profiles obtained from 900 m pathlength FT-IR spectra of Riverside ambient air on October 14, 1977 .	30
12	Distribution of simultaneous observations of ammonia and nitric acid concentrations	32

FIGURES

Number		Page
13	Logarithm of the NH_3-HNO_3 concentration product vs. the reciprocal absolute ambient temperature.	33
14	Concentrations of ozone and other pollutants in photochemical smog measured at Claremont, California, October 1978	35
15	Single beam spectra showing the concentration levels of nitric acid (HNO_3) and formaldehyde (HCHO) during the severe smog episode of October, 1978, Claremont, California	37
16	Regression fits of the FT-IR HNO_3 data with those obtained by the BAT/CHEM and BNL/HVF methods.	47
17	Regression fits of the FT-IR HNO_3 data with those obtained by the EPA/NTR and NCAR/LVF methods.	48

TABLES

Number		Page
1	Calculated Detection Limits for Several Pollutant Species. . .	16
2	Maximum Pollutant Concentrations (ppb) Measured in Riverside Air in 1977.	29
3	Thermodynamic Data for the NH_4NO_3 Equilibrium at 306.6 K . . .	34
4	Daily Maximum Concentrations (ppb) Observed in Claremont, California by Kilometer Pathlength FT-IR Spectroscopy. . . .	36
5	Methods for Measurement of Nitric Acid and Particulate Nitrate.	42
6	Nitric Acid and Particulate Nitrate Sampling Schedule	43
7	Ancillary Measurements for the Nitric Acid/Particulate Nitrate Field Study.	44
8	Results of Nitric Acid Measurements.	46
9	Regression Fits for Nitric Acid with the FT-IR Data as Standard.	49

ACKNOWLEDGEMENTS

The design, fabrication, and initial assembly of the kilometer pathlength FT-IR facility employed in this study was carried out by Dr. Philip L. Hanst of the Environmental Protection Agency. We are also indebted to Dr. Hanst for his contributions as Project Officer during the first two years of this program and for his sustained interest in the project throughout its duration. We gratefully acknowledge the cooperation and assistance of Mr. Bruce W. Gay, Jr. and Mr. John W. Spence, each of whom subsequently served as Project Officers for intervals of this program.

We wish to thank Mr. Ron Easton and Mr. Richard Brown for their valuable assistance in conducting the experimental program, and Ms. Yvonne Katzenstein for her contributions as technical editor of this report.

The assistance of Professor Gregory Kok and Dr. Kenneth Baker, President of Harvey Mudd College, in arranging for the siting of the kilometer pathlength facility on the roof of the Jacobs Science Center on the Harvey Mudd College campus in 1978 and 1979 is gratefully acknowledged.

SECTION 1

INTRODUCTION

During the past decade, the major efforts of federal, state and local agencies in the acquisition of an air monitoring data base have been largely focused on the regulated or "criteria" pollutants, i.e., ozone (O_3), nitrogen dioxide (NO_2), total hydrocarbons, sulfur dioxide (SO_2) and total suspended particulates (TSP). At the same time, laboratory and smog chamber studies, as well as the more comprehensive computer kinetic models of photochemical air pollution which were being developed (1-8), increasingly stressed the importance of a number of trace species and their roles in photochemical air pollution. These important species include formaldehyde (HCHO), formic acid (HCOOH), nitric acid (HNO_3), nitrous acid (HONO), hydrogen peroxide (H_2O_2), and the nitrate radical (NO_3), as well as ammonia (NH_3). Until recently, comparatively little progress had been made in characterizing the concentration ranges and the temporal and geographical distributions of these significant, but presently unregulated, air pollutants.

Prior to the work reported here, the lack of data concerning the ambient concentrations of many nitrogenous and oxygenated compounds had focused considerable attention on the few reported measurements for some of these species. Thus, the Fourier transform infrared (FT-IR) study in 1973 by Hanst and co-workers (9), in which formic acid was observed spectroscopically in ambient air for the first time, the measurement of ambient nitric acid concentrations by Spicer and Miller (10,11) using a modified Mast coulometric technique in 1972-1974, and the Harvey Mudd College/University of California, Riverside-Statewide Air Pollution Research Center (UCR-SAPRC)/ Environmental Protection Agency (EPA) collaborative measurements (12) of ambient hydrogen peroxide in the California South Coast Air Basin attracted widespread interest. These studies were virtually the sole additions to the published scientific literature concerning the atmospheric presence of these

species since the wet chemical technique studies by Mader et al. in 1955 for formic acid (13), by Altshuller and McPherson (14) in 1963 for formaldehyde, and by Gay and Bufalini (15) for hydrogen peroxide in 1971. Thus, the recently revised air quality criteria document for oxidants (16) lists fewer than a half-dozen ambient air studies in which these or related species were measured.

The lack of data concerning the ambient concentrations of the so-called "non-criteria" pollutants is striking in view of their potential importance to atmospheric chemists and modelers, to control officials, and to others who are concerned with impacts on agriculture and human health. To cite only a few examples:

- A number of computer kinetic models of photochemical smog formation (17,18) now incorporate aldehyde mechanisms; in particular the role of formaldehyde as an initiator of photochemical smog reactions is well established. However, data concerning ambient concentrations of formaldehyde in urban atmospheres (including diurnal variations in its concentration) have not been available as inputs to such air shed models (19).
- Dawson (20) has pointed out that the sources and sinks of atmospheric ammonia have been largely ignored in the recent concern over the role of oxides of nitrogen in the chemistry of the upper and lower atmosphere, and states: "This neglect is somewhat surprising, since ammonia occupies a singularly pivotal position in the system, having importance in each of the domains separately. The absence of a rapid and reliable instrument for the detection of low ammonia levels may be largely at fault."
- Reports of eye irritation in locations such as the California South Coast Air Basin have decreased markedly over the past 15 years; due to the lack of a data base for trace pollutants which may be eye irritants or precursors to eye irritants, it is difficult to definitively attribute this decline to the reduction of vehicular emissions or to the control of stationary source emissions of reactive organics.
- It is well established (21,22) that the commercial chemiluminescent analyzers for NO_2 which are now in widespread use in air moni-

toring networks throughout the U. S. are subject to a quantitative interference by nitric acid, peroxyacetyl nitrate (PAN), alkyl nitrates, and other nitrogenous compounds. In some cases, these interferences could lead to serious errors in reported versus actual NO_2 concentrations in the air monitoring data base. Unless representative data are available concerning the ambient levels of species such as nitric acid, it is difficult to assess the possible magnitude of these errors.

- Newly characterized compounds such as peroxynitric acid (HO_2NO_2) (23-29) and alkylperoxy nitrates (RO_2NO_2) (30-32) have been recently observed in laboratory studies by a number of workers, but there is a complete lack of experimental information concerning their possible presence in ambient air, although their ambient concentrations, as inferred from laboratory and modeling data, are likely to be very low, i.e., $\lesssim$1 ppb (7,8).
- Baseline data are needed for anticipated future atmospheric pollutants which are not now being monitored. For example, the launching of space shuttles from Vandenburg Air Force Base in southern California as often as several times each month in the 1980's is expected to inject some 30 tons of HCl below the inversion layer for each launch (33). It would appear prudent to determine present ambient levels of HCl for comparison with levels observed when the space-shuttle program is fully operational.
- Although ammonia and nitric acid are believed (34,35) to react to form visibility-reducing ammonium nitrate aerosol in photochemical smog, data concerning the concentrations of NH_3, HNO_3 and NH_4NO_3 coexisting in ambient air have been generally unavailable.

These and related needs for ambient air measurements of trace pollutants in photochemical smog led us in 1976 to initiate such measurements under an Environmental Protection Agency (EPA) sponsored program employing a kilometer pathlength FT-IR spectrometer originally designed and assembled by Dr. P L. Hanst of the EPA-Research Triangle Park (RTP) Laboratories. This system provides an <u>in-situ</u> part per billion (ppb) detection capability for many oxygenated and nitrogenous pollutants for which reliable, alternative

analytical methods are presently unavailable, or are only now being developed. We report here the results of this four-year program.

SECTION 2

BACKGROUND

A. Historical Role of Long-Path IR Spectroscopy in Air Pollution Research

The initial applications of long-path infrared (LPIR) spectroscopy to the identification and quantitative measurements of pollutants in atmospheric and synthetic smog systems were carried out by Stephens, Scott, Hanst and Doerr (36-39) at the Franklin Institute between 1953 and 1957. These studies employed a prism spectrometer (equipped with thermocouple detectors) interfaced to a White-type multiple reflection cell (40) operated at pathlengths between 40 and 400 meters. Among the most significant contributions made with this technique were the first spectroscopic proof of ozone formation (36) in photochemical smog and the discovery of the highly toxic secondary pollutant peroxyacetyl nitrate (PAN) (36,37,39), a compound unknown to chemists prior to its characterization in photochemical smog by LPIR spectroscopy. Other early spectroscopic applications included studies of irradiated auto exhaust (41), plant damage (42), hydrocarbon reactivity (43,44) and ozone-olefin reactions (38,45). Some later studies, employing grating monochromators and high-performance cooled detectors, dealt with calibration techniques for ozone (46-48).

The applicability of the LPIR method to a wide range of atmospheric and laboratory studies results from several important strengths of this technique, the most significant of which are (a) its specificity, (b) its nondestructive and quantitative nature, and (c) its potential for detection of relatively low concentrations of species with good time resolution. This potential has been realized in recent years due to two important advances in technique: first, the advent of high resolution, rapid scan, Fourier transform infrared (FT-IR) spectrometers, and second, the development of multiple-reflection optics of greater total pathlengths. Thus, recent studies employing FT-IR instruments interfaced to long-path optical

systems include investigations of products from ozone-olefin systems (49-50), nitrous acid equilibria (51), oxidation of chlorinated ethylenes (52), and characterization of novel species such as peroxynitric acid (23,25-27,29) and its alkyl-substituted homologs (30-32).

B. Background to Present Study

The application of FT-IR spectroscopy to measurements of trace levels of pollutants in the real atmosphere was pioneered by Hanst and his co-workers (53,54). The forerunner to our present research program was a program conducted by Hanst, Wilson, Patterson, Chang and Burton (9) in Pasadena, California, during November, 1972, and July-August, 1973. In that study, a Digilab Fourier Transform Spectrometer and a folded-path optical system (with a base path of 8.7 m) being operated at total path-length of 417 m were employed on the roof of the Keck Engineering Building at the California Institute of Technology. Formic acid was observed spectroscopically in ambient air for the first time and low upper limits were set for the presence of HNO_3, N_2O_5 and alkyl nitrates ($\leq$10 ppb) and for formaldehyde ($\leq$30 ppb).

Subsequently, a new LP-IR spectrometer system, capable of extending pollutant detection to still lower concentration regimes, was developed by Hanst at the EPA-RTP Laboratories. The system consists of a Digilab FTS-14 spectrometer with data system and peripherals and a 22.5 m base-path, multi-pass optical system capable of total pathlengths as long as 2 km. In 1976 this system was eventually modified and set up for field studies in the California South Coast Air Basin by the UCR-SAPRC research team and the four-year program of ambient measurements described in this report was conducted.

SECTION 3

INSTRUMENTATION AND METHODS

A. Description of the FT-IR Spectrometer and Kilometer-Pathlength Cell

Figure 1 illustrates the eight-mirror multiple reflection optics employed in this study. The details of its design have been described by Hanst (53). The in-focus (nesting) mirror assembly consists of four rectangular mirrors, three of which measure 6.4 cm x 32 cm, while the fourth is slightly shorter to provide the entrance and exit apertures for the infrared beam. The out-of-focus assembly (collecting mirrors) consists of four 30 cm diameter mirrors and is 22.5 m (the average radius of curvature of the eight mirrors) from the nesting mirror assembly. All mirrors are optically polished and gold-coated for maximum reflectivity in the infrared. The sequence of reflections are shown by numbered dots in Figure 1. The number of images is varied by the lateral adjustment of mirror C4. The six images shown for the mirrors N1, N2 and N3 represent a pathlength equal to 6 x 8 x 22.5 = 1080 m (~1 km).

The cell consists of a sectional rectangular aluminum frame (total dimensions: 0.81 x 0.84 x 23 m) with a lining of 50-micron thick FEP Teflon film. Teflon was chosen to provide a relatively inert, replaceable surface, as well as for its good transmission of solar radiation when the cell is being used alternatively as a reaction chamber for synthetic systems. A removable sun screen can be installed over the entire length of the cell to reduce thermal effects on the stability of the infrared beam during ambient monitoring. To minimize vibrations, the mirror assemblies are each mounted on platforms completely independent of the cell housing.

Figure 2 depicts the multiple-reflection cell coupled to the Fourier transform spectrometer system, which is housed in a 3.7 x 3.7 m air-conditioned building. The collimated infrared beam from a Nernst glower is modulated by a Digilab Model 296 Michelson IR interferometer (resolution

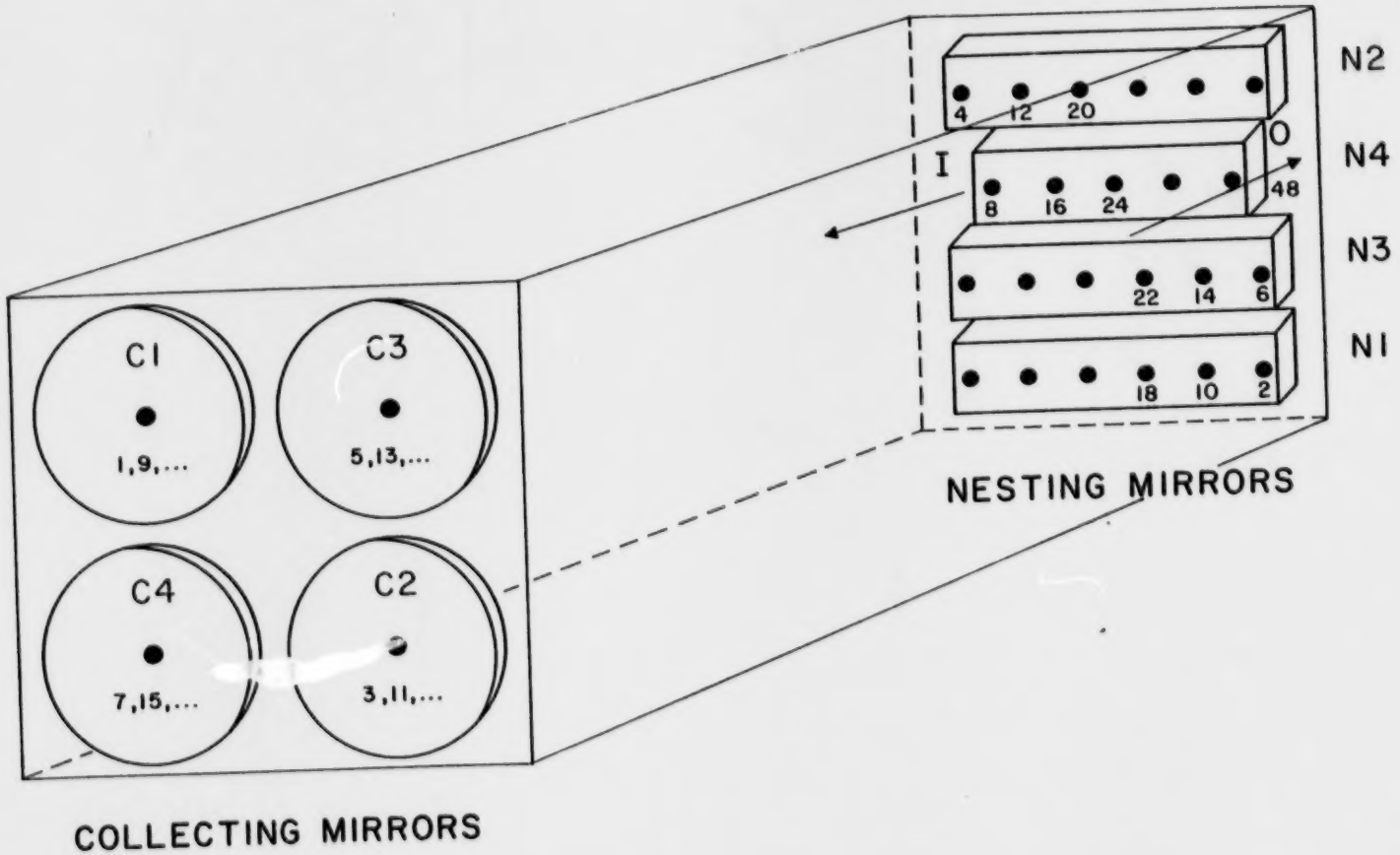

Figure 1. Eight mirror multiple reflection system. Numbered dots indicate sequence of reflections during six complete passes through the cell; I = entrance aperture; 0 = exit aperture.

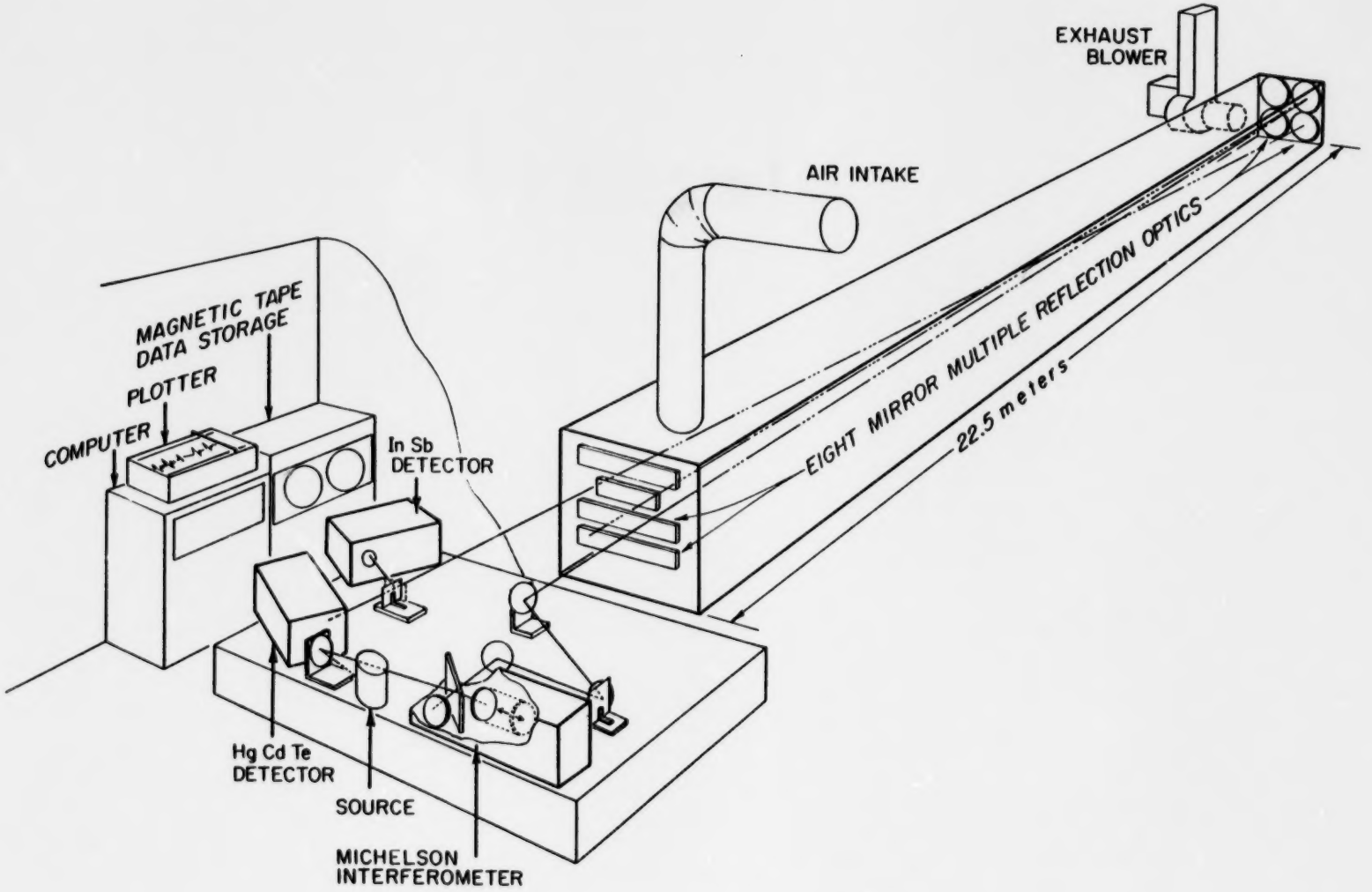

Figure 2. Kilometer pathlength FT-IR system.

$\geq$0.5 cm^{-1}) and a magnified image of the source element is focused at the entrance aperture of the cell. The beam exiting from the cell is sent to either of two liquid-N_2 cooled detectors: a photovoltaic InSb detector for the 2000 to 4000 cm^{-1} range or a photoconductive HgCdTe detector for the 600 to 2000 cm^{-1} region. A two-position mirror permits alternate imaging on the two detectors.

Data collection and processing are performed by a Data General Nova 1200 computer with 4096 16-bit words of core. A disk unit (128 K words) is used for software storage and partial storage of data. Archival data storage of both raw interferograms and computed spectra is provided by a Kennedy Model 9700 magnetic tape unit. The Digilab system is also equipped with a pen plotter, an oscilloscope and a teletype.

B. Operation of the Long-Path FT-IR System

During a scan of the interferometer mirror, an audio-frequency sinusoid is generated for each infrared frequency element. The interferogram is the summation of all such sinusoids from the whole range of incident optical frequencies and is related to the actual spectrum (radiation intensity vs. wavelength) by the Fourier transform. Thirty or forty such interferograms were usually co-added to enhance the signal-to-noise ratio in the interferogram, and thus in the computed spectrum. The spectral resolution routinely employed was 0.5 cm^{-1} with 16384 digitized points in each interferogram. At this resolution the vibration-rotation structure of most light molecules present in the ambient air sample can be resolved and used for positive identification.

The sampling procedure consisted of drawing air into the cell at a rate of 330 liters sec^{-1} for a minimum of four minutes before the start of an interferometer scan. This corresponded to a displacement of the previous air sample by a minimum of five volumes of fresh sample. A total pathlength of 900 meters and a resolution of 0.5 cm^{-1} were employed. Actual data collection of 30 co-added interferograms took no more than six minutes. Data collection, transform computation, and routine plotting of a portion of the spectrum and magnetic tape storage could be accomplished within 10 minutes for each detector. Hence, a time resolution of three complete spectra (600-4000 cm^{-1}) per hour, using both HgCdTe and InSb detectors, is available to characterize moving smog fronts.

C. Spectral Processing

Strong absorptions due to the H_2O and CO_2 content of the atmosphere render certain regions of the infrared unsuitable for detection of pollutant molecules. At pathlengths of 1 km and longer, the spectral windows for infrared detection are generally limited to the 760-1300 cm^{-1}, 2000-2230 cm^{-1} and 2390-3000 cm^{-1} regions. This means that some characteristic functional group absorptions, such as those due to stretches of the C=O, C=C and O-H bonds, generally cannot be employed. Nevertheless, the majority of pollutant molecules have "fingerprint" absorptions in the accessible infrared regions. For data analysis the spectra are retrieved from storage and ratioed against a clean background spectrum with the same water content in order to eliminate the majority of interfering water absorptions and to facilitate the measurement of band intensities. A limited amount of arithmetic manipulation of the available background spectra can be used to improve the matching of the water content.

D. Detailed Considerations Pertaining to Optimum Instrument Performance and Accuracy of Spectral Data

1. Optical Components and Alignment

In addition to the general alignment procedure described above, steps were taken to identify and eliminate stray radiation from the cell optics that could impinge on the detector and cause photometric errors. (The effect of the stray irradiation is similar to the photometric inaccuracy that is introduced by light leakage around the sample, e.g., KBr pellet, in the more conventional applications of analytical spectroscopy.) The stray radiation in the beam leaving the cell results from the primary beam overfilling mirror C1 and striking mirrors C2 and C3 (see Figure 1). It was eliminated by masking a small portion of the parallel beam output of the interferometer.

The collimated beam input to the interferometer was verified to be in exact coincidence with the optical axis by observing that the return beam from the quartz beamsplitter was focused back on the source element. A significant deviation of the input beam from the optical axis would result in appreciable degradation in resolution and shift in the spectral frequency.

Channel spectra ("fringing") which initially interfered in the absor-

bance measurements were identified as originating from the windows originally used for the detector dewars. For the HgCdTe detector, the channel spectra were eliminated by substituting a wedged Ge window which, additionally, has a filter coating with a short wavelength cut-on at 5 μm (2000 cm^{-1}). For the unremovable sapphire window of the InSb detector, the problem was corrected by directing the infrared beam onto the external filter (cut-on point ~2.5 μm) and detector element at the minimum angle for which channel spectra were not detectable. The filter characteristics were effective in eliminating spectral folding ("aliasing") at the sampling interval and bandwidth (based on the He-Ne laser wavelength) employed during data collection.

Since the cell mirrors were constantly exposed to air pollutants, including aerosols and dust particles, the gold coatings were periodically inspected and washed with 95% ethanol. The mirrors were re-coated at the start of each monitoring (smog) season.

2. Ambient Air Sampling

The choice of sites for the FT-IR facility were made such that no potential source of interfering primary pollutant emissions were present in the immediate vicinity. The capacity of the blower (330 liter sec^{-1}) which drew air through the cell and the sampling times chosen ensured that a displacement of the previous air sample by $\geq$5 volumes of fresh sample was attained.

During the first year of this study, data collection was carried out with air samples being drawn continuously through the cell. This procedure was utilized in the relatively few smog episodes recorded during that period, despite our recognition that this sampling method introduced additional noise in the spectra. This was necessary since the low incidence of pollution during the fall of 1976 prevented us from conducting an adequate number of experiments that would establish the loss rate of secondary pollutant species when sampling was suspended while spectra were being recorded. Several such experiments were carried out during the following summer. Spectra were recorded while polluted air was drawn continuously through the cell and then while the system was in the stopped flow mode. These experiments established that there were no significant losses of key pollutant species (e.g. HCHO, HNO_3, HCOOH) to the cell walls during the

brief ~6 minutes) scanning period. An intermittent sampling mode was therefore adopted for the remainder of the study.

3. Spectral Analysis

Even at the highest spectral resolution (0.5 cm^{-1}) afforded by the instrument employed in this study, nearly all of the infrared analytical bands of the pollutant molecules of interest suffer to a greater or lesser extent from interferences by atmospheric H_2O and CO_2 absorptions. Where applicable, the absorbance measurements were derived from the intensities of the "Q-branch" features only, in order to minimize the effect of baseline distortion arising from inexact cancellation of H_2O absorptions and possible interferences by broad absorptions of unidentified species.

The accuracy of the absorbance measurements also depends to a large extent on the "purity" of the reference spectra employed to obtain ratio plots. Most of the air reference spectra used during the studies in Riverside were conveniently generated from SAPRC's air purification system (55) which has the additional capability of controlled humdification of the air output. Additional reference spectra, which were needed during operation at locations other than UCR, were obtained by humidifying N_2 gas which was vaporized from a tank of liquid nitrogen.

Although the reference spectra employed were satisfactory for certain infrared regions, their use in other spectral regions entails additional corrections for CO_2 and CH_4 absorptions. These interfering absorptions result from the much lower CO_2 and CH_4 content of the purified air compared to that of ambient air. In particular, the two groups of CO_2 "laser lines" centered at 961 and 1064 cm^{-1} interfere with the measurement of NH_3 and O_3, respectively. Therefore, the pure-air reference spectra were supplemented by others obtained from ambient air samples.

The latter were obtained on days of low pollution by drawing ambient air into the cell through a humidification chamber (utilizing the flow of water through spray nozzles) attached to the air intake. These ambient air reference spectra were then characterized with respect to possible traces of pollutants by comparison with the humidified N_2/pure air reference spectra. Interferences due to mismatch of the CO_2 content were generally negligible when ambient air reference spectra were employed to

interpret spectra taken during smog episodes. Some of the reference spectra were intended specifically for the analysis of a single species.

E. FT-IR Absorptivities and Detection Limits

Our initial estimates of pollutant concentrations in the first year of this study were based on literature values of absorptivities which were measured at lower spectral resolutions ($\geq$2 cm^{-1}) than those employed in this program. Estimates of the absorptivities at 0.5 cm^{-1} resolution were obtained by multiplying the literature values by the ratio of the peak height at 0.5 cm^{-1} resolution to that at lower resolution (as generated by the smoothing function provided in the Digilab software). We have since made new measurements of absorptivities for several of the compounds of interest in this study and in some cases have found significant disagreements with the literature values. For example, the values for the 1105 cm^{-1} absorption of HCOOH (Q branch height only) were measured in our laboratory to be 70, 64 and 50 cm^{-1} atm^{-1} at resolutions of 0.5, 1 and 2 cm^{-1}, respectively. By contrast, the value reported by Hanst et al. (9) at 2 cm^{-1} resolution is only 13 cm^{-1} atm^{-1}, almost a factor of four lower than our measured value.

The new measurements of absorptivities for HCOOH, HCHO, NH_3 and HNO_3 were carried out in the SAPRC evacuable chamber (56) which is equipped with White cell optics. Spectra recorded with an Eocom interferometer provided resolutions of 0.125 and 1 cm^{-1}. Different concentrations (at ppm levels) and pathlengths (10-40 meters) were employed at these two resolutions for each compound. Corrections were made for the observed decreases in concentration due to adsorption on the chamber walls ($\leq$5% per hour). The absorptivities for 0.5 and 2 cm^{-1} resolutions were derived from the 0.125 and 1 cm^{-1} spectra using in-house software (57) which employed a sin(x)/x smoothing function to generate the lower resolution spectra.

The spectra obtained by FT-IR spectrometers may be evaluated by various methods. The discrete data points calculated by the Fourier transform from the minimum-sized interferogram for a given resolution all have unique information content. For instance, for our 1 cm^{-1} spectra the data points are 0.5 cm^{-1} apart. When the width of an absorption feature is comparable to the spectral resolution, these data points may not

fall near the feature's region of maximum absorption. The absolute spectral positions of these points are very reproducible between spectra and between rapid-scan interferometers since most current systems use a He-Ne laser for reference and use phase correction in their calculations. Although the interpolation of additional plotted points (using an appropriate function to match the instrumental line-shape, such as sin(x)/x) will give a "true" total peak height for the given spectral resolution, this procedure is too time-consuming for most work. Hence, the pollutant absorptivities we report here are for spectra containing only the minimum number of data points for the given resolution. When a spectrum is smoothed by a factor of two, therefore, only the even numbered data points are retained in order to preserve data compatibility with spectra taken at the lower resolution. This method of smoothing was found to give peak heights at the reduced resolutions nearly equivalent to those obtained from the spectra calculated from smaller interferograms.

The resolution dependence of the absorptivity values measured with our Eocom interferometer system was subsequently tested in the Digilab-equipped kilometer-pathlength FT-IR system. Samples of HCOOH, HCHO and NH_3 sufficient to yield 10-20% absorption for the analytical peaks at a 1 km pathlength were introduced into the sealed cell through a Teflon disperser tube running the length of the cell. Spectra for each compound were alternately recorded at 1 cm^{-1} and 0.5 cm^{-1} resolution over the course of a two hour period. Parallel curves of absorption versus time for these two resolutions were obtained to compensate for possible loss of the compound due to cell leaks and wall adsorption, as well as possible sample inhomogeneity. The absorption ratios obtained for the analytical peaks at 0.5 cm^{-1} to those at 1 cm^{-1} resolution confirmed that the 0.5 cm^{-1} absorptivities derived from the laboratory measurements at other resolutions are correct. These results also brought out the inaccuracy of the Digilab smoothing function for generating lower resolution spectra. For example, with this function ratios of the 1105 cm^{-1} Q branch absorption of HCOOH for different resolutions are $A_{0.5}/A_{1.0} = 1.6$ and $A_{0.5}/A_{2.0} = 2.2$, whereas the correct ratios are 1.1 and 1.4, respectively.

Table 1 gives the absorptivities which we have determined for HCOOH, HCHO, NH_3 and HNO_3 along with the corresponding detection levels for these

TABLE 1. CALCULATED DETECTION LIMITS FOR SEVERAL POLLUTANT SPECIES

Compounds	Measurement frequency (cm^{-1})	Absorptivities* (cm^{-1} atm^{-1}, RTP)	Resolution (cm^{-1})	References	Approximate detection limit (ppb) at 1 km path
O_3	1055	9.7	1-2	(Pitts et al., 1976, ref. 47) (McAfee et al., 1976, ref. 48)	10
PAN	1162	32	2-4	(Stephens, 1964, ref. 58)	3
NH_3	931	27	0.5		4
	967.5	35	0.5	This work	3
	993	21	0.5		4
HNO_3	896	12	0.5	This work	6
HCHO	2779 2781.5	16	0.5	This work	6
HCOOH	1105	70	0.5	This work	2
HONO	791 (trans)	~30	0.5		10# (cis + trans)
	853 (cis)	71	0.5	(Chan et al., 1976, ref. 51)	
H_2O_2	1250	8.4	1-2	(Molina & Molina, 1980, ref. 59; Hanst et al., 1975, ref. 9)	40#
$HOONO_2$	803	27	0.5-1	(Graham et al., 1977, ref. 27)	8#

* = $\ln(I_o/I)/pl$

~23°C, 760 torr

Measured from the intensity of the Q branch only (see text).

#See text for discussions of atmospheric interferences for the spectral analysis of HONO, H_2O_2, and $HOONO_2$ concentrations.

compounds in the present system at a 1 km pathlength. For the analytical bands of HCOOH at 1105 cm^{-1} and HCHO at 2780 cm^{-1}, no more than 10% difference exists between the absorptivity value of the Q-branch height alone and that of the total value as measured from the true baseline. For HNO_3, however, the total absorptivity at 896 cm^{-1} is approximately twice that of the value for the Q feature alone due to the significant contribution of the broad P and R branches. We have verified that the Q branches obey Beer's law for our experimental conditions and have been adopted for our measurements of the above compounds.

The detection limits given in Table 1 are, in most cases, based on a 1% absorption. For the 993 cm^{-1} line of NH_3 and the 896 cm^{-1} Q-branch of HNO_3, however, the detection sensitivities are slightly better (~0.75% absorption) because these features are minimally interfered with by atmospheric H_2O and CO_2 absorptions. Our analysis of a great number of spectra from the 1977 program also allowed us to establish operational minimum signal levels at which H_2O_2, HONO and $HOONO_2$ can be positively detected. The interferences and the estimated detection limits for these species are discussed in later sections.

SECTION 4

MEASUREMENT OF POLLUTANTS IN AMBIENT AIR

During the first two years (1976 and 1977) of this study, the FT-IR spectrometer and kilometer-pathlength cell were operated in Riverside, approximately 60 miles east and 8-12 hours downwind of the primary emission sources in the California South Coast Air Basin. The facility was moved to Claremont, a mid-point site between Riverside and the Los Angeles metropolitan area, for studies covering the smog seasons of 1978 and 1979. The findings of the studies in Riverside have already been published (60,61) and only brief discussions of the significant results will be presented here. The unpublished data of the Claremont studies will be dealt with more thoroughly in this report.

A. First Year of Study

The initial phase of this study was started in July 1976 with assembly of the instrumentation on the roof of the Webber Hall East building on the UC Riverside campus. This location is 24 m above ground and provides unobstructed exposure to prevailing winds from the west, north or south. Modification of the cell (i.e., the use of Teflon film in the place of the original Plexiglass walls), extensive testing of the spectrometer system, and development of routine operating procedures were conducted during this period.

Due to unusual meteorological conditions, a very low incidence of pollution episodes was experienced in Riverside during the summer and fall of 1976. Our monitoring efforts succeeded in recording only three moderate smog episodes which occurred on October 4, 5 and 6, 1976. Nevertheless, the initial study provided valuable benchmark data and yielded significant results.

Spectra representing detection of NH_3, HCHO and HNO_3 in Riverside air are given in Figures 3-5. Reference spectra for comparison are pre-

sented in Figure 6. To the best of our knowledge, these first year results in Riverside represented the first direct spectroscopic detection of HNO_3 and HCHO in the atmosphere. The previously suspected prevalence of relatively high levels of NH_3 in Riverside, originating primarily from upwind agricultural sources, was confirmed in our measurements.

The concentration vs. time data for O_3, PAN, NH_3, HNO_3, HCOOH and HCHO obtained for the three episode days of October 4, 5 and 6, 1976 are given in Table A-1 of Appendix A. The data have been re-analyzed for NH_3, HNO_3, HCOOH and HCHO to be consistent with our latest absorptivity measurements for these compounds; thus, the values in Table A-1 differ from those reported in an earlier publication (60). In particular, the HCOOH concentrations drastically changed as the literature value of the absorptivity (9) on which the earlier estimates were based was found to be seriously in error (c.f. section on FT-IR Absorptivities and Detection Limits). The data for the above compounds, as presented in Table A-1, though significant, are to be considered as exploratory results. For applications to chemical modeling, the more accurate and extensive results of the succeeding studies in Riverside and Claremont should be utilized.

The usefulness of the present long-path FT-IR set-up as an independent check on the accuracy of dedicated monitors for specific species was first applied to a comparison of ozone readings with a Dasibi continuous analyzer. The latter instrument had been previously calibrated, by means of a transfer standard, against a 1 m UV spectrophotometer at the California Air Resources Board Laboratory in El Monte. FT-IR measurements of O_3 concentrations were made from the R-branch absorption at 1055 cm^{-1} (Figure 7). Results from simultaneous measurements on October 4-6 of ambient O_3 concentrations (in the 50-300 ppb range) by the two methods are plotted in Figure 8. The FT-IR measurements averaged 0.9% higher than the averaged Dasibi readings for the same time period, and the standard deviation of the percentage differences was 4%. Thus, excellent agreement was obtained between the two methods.

It was originally proposed that the FT-IR system also be used in the characterization of halocarbon levels in the atmosphere. Indeed, $CFCl_3$ and CF_2Cl_2 were observed in several of our measurements but at erratic levels, ranging from near detection limits (< 1 ppb) to highly

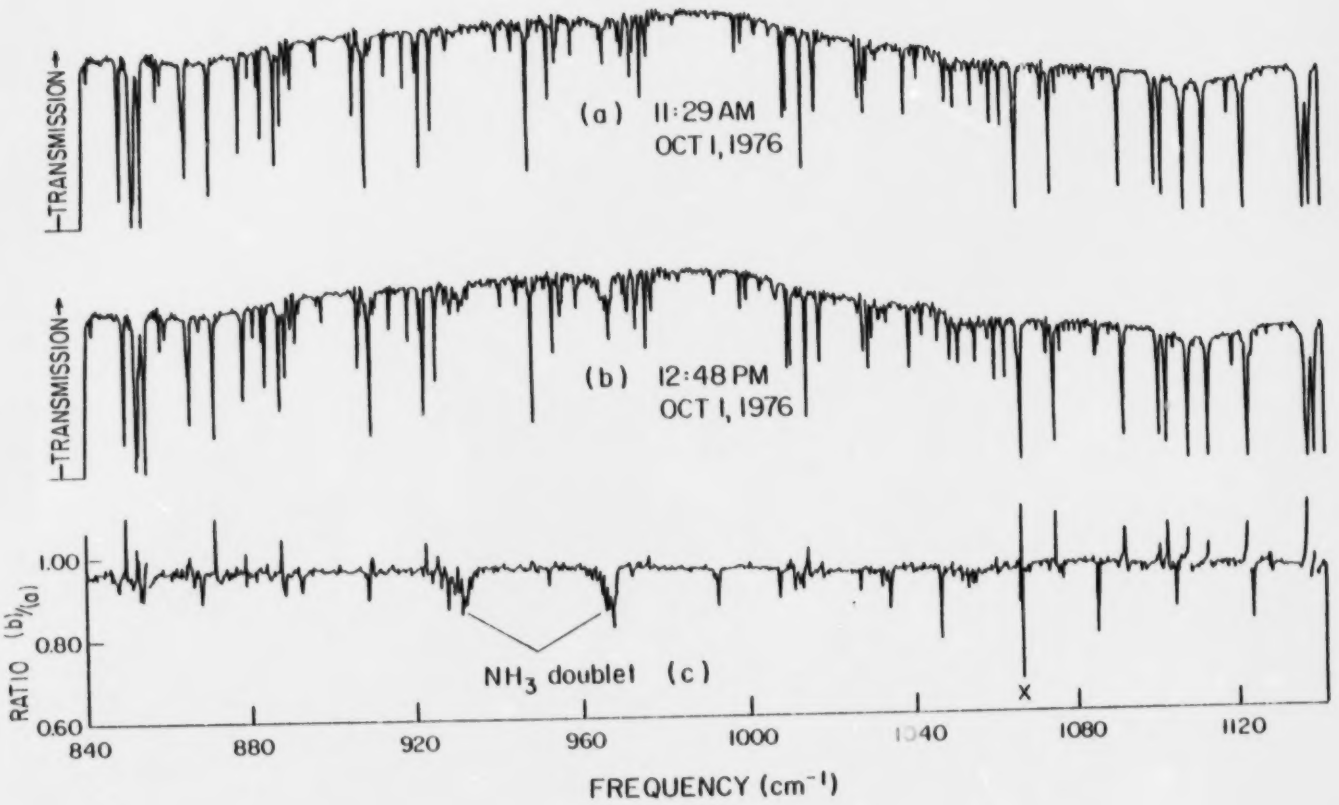

Figure 3. Riverside ambient air spectra at 0.5 cm^{-1} spectral resolution, 1080 m pathlength. NH_3 concentration, 44 ppb.

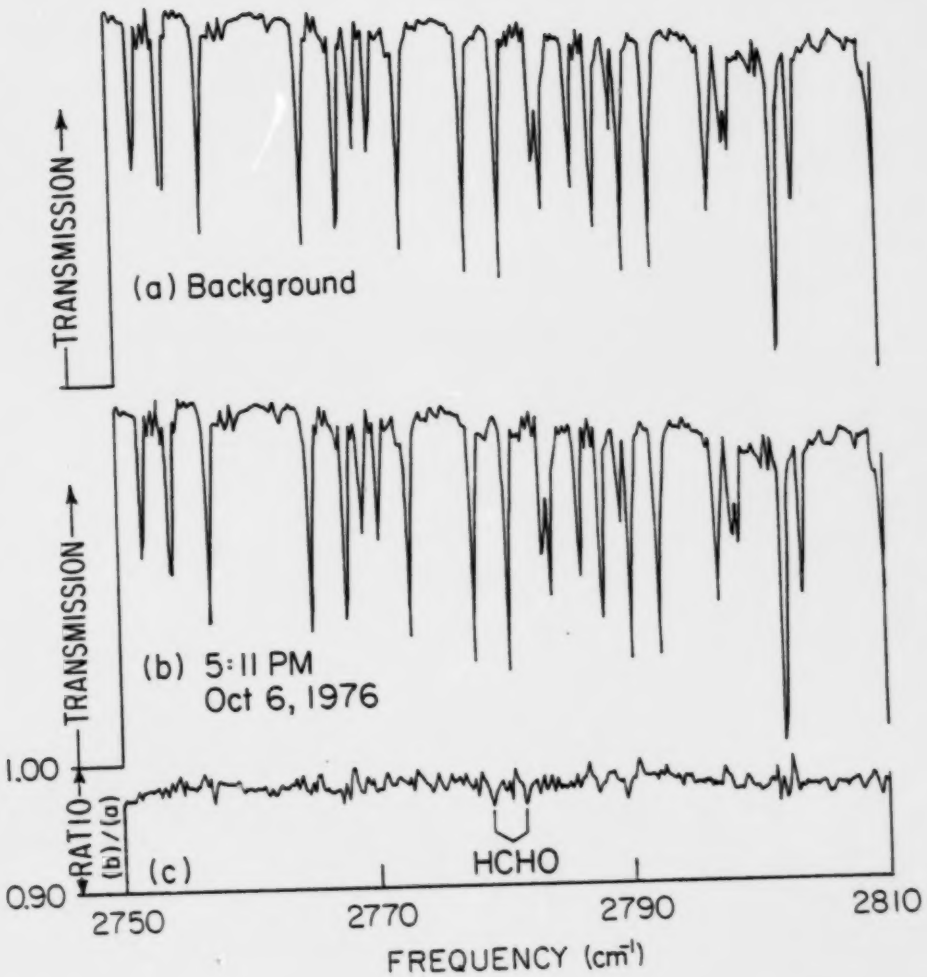

Figure 4. Riverside ambient air spectra at 0.5 cm^{-1} spectral resolution, 1080 m pathlength. Formaldehyde concentration, 11 ppb.

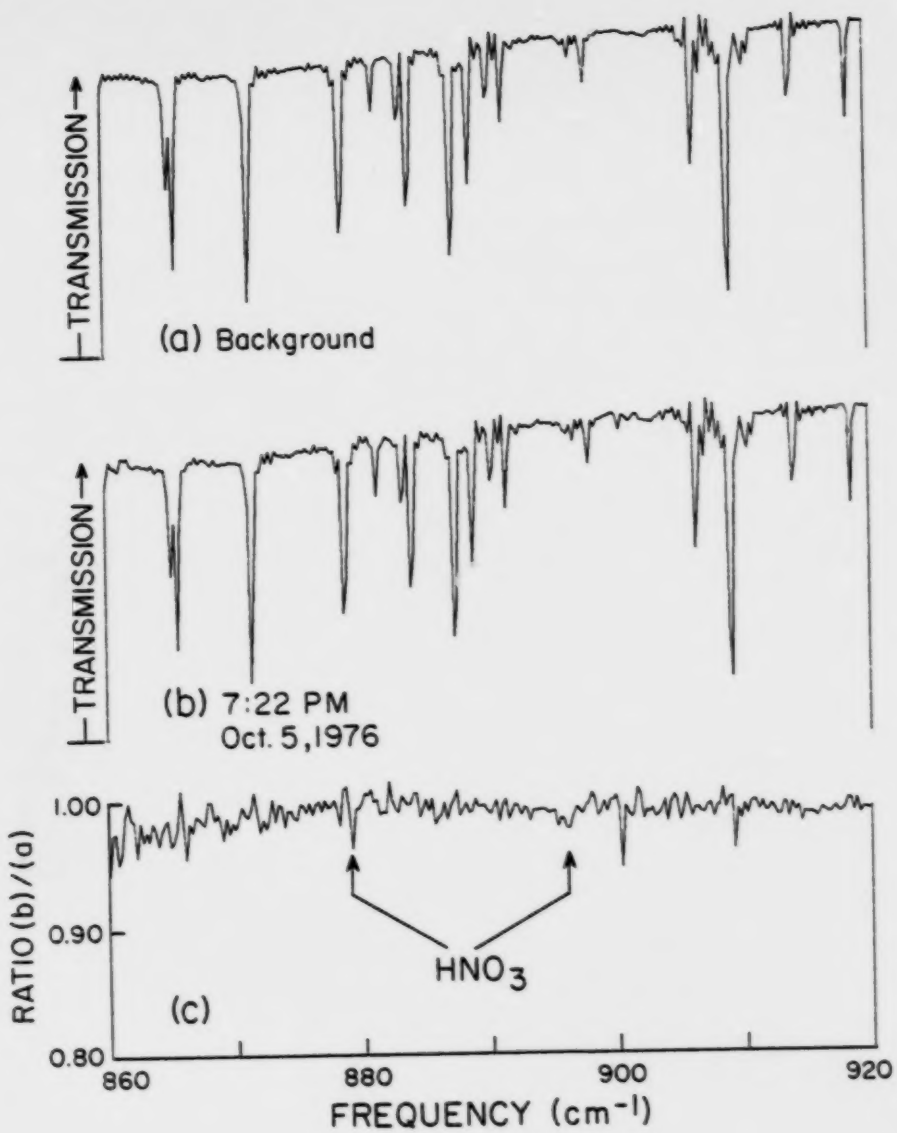

Figure 5. Riverside ambient air spectrum (October 5, 1976 at 7:22 p.m.) at 0.5 cm^{-1} spectral resolution, 1080 m pathlength. Nitric acid concentration, 8 ppb.

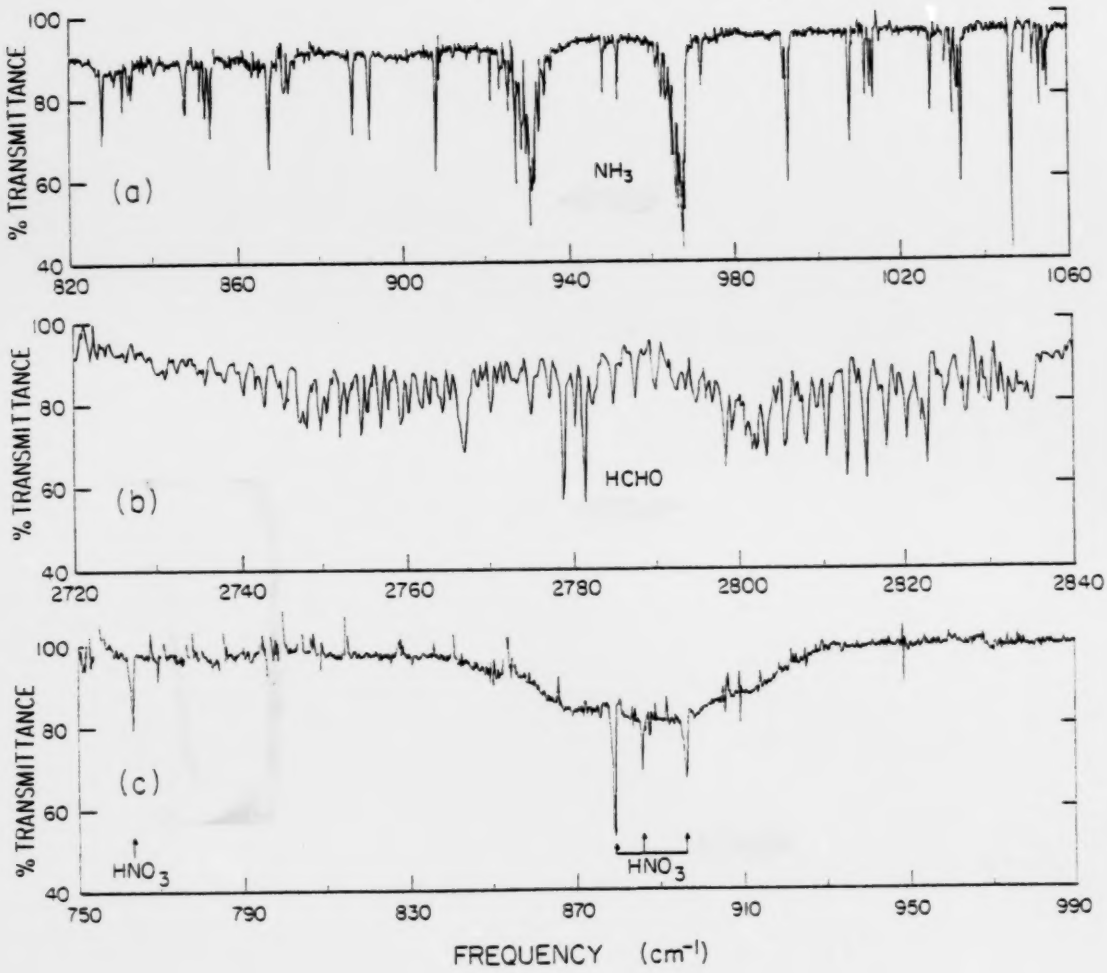

Figure 6. Reference spectra at 0.5 cm^{-1} spectral resolution and 1080 m pathlength: (a) ammonia, ~200 ppb; (b) formaldehyde, ~270 ppb; (c) nitric acid, ~150 ppb.

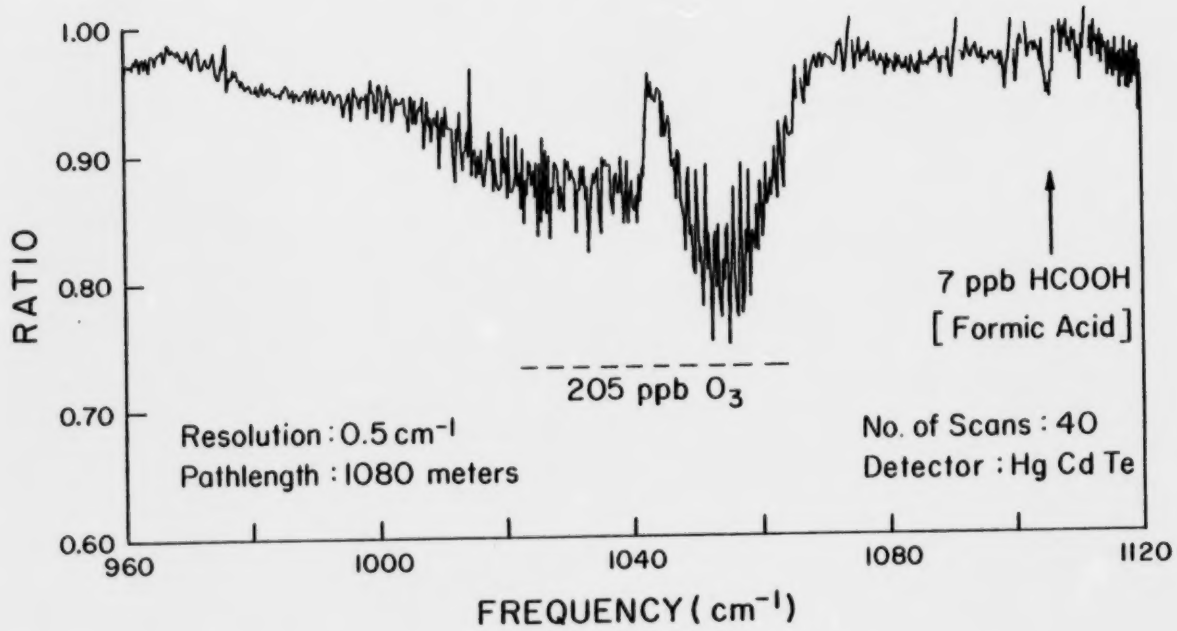

Figure 7. Riverside ambient air spectrum (October 5, 1976 at 6:33 p.m.) at 0.5 cm^{-1} spectral resolution, 1080 m pathlength. Formic acid, 19 ppb; ozone, 205 ppb.

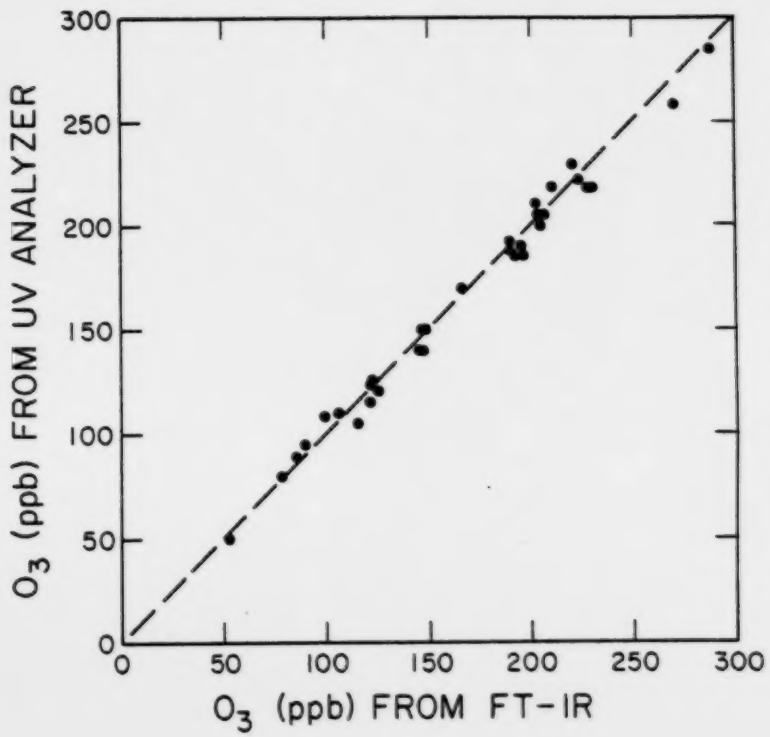

Figure 8. Comparison of FT-IR and UV analyzer measurements of ambient ozone concentrations.

unrepresentative levels of several tens of ppb at certain times in the summer. (The latter values were traced to breakdowns of refrigeration units on the UCR campus.) After some initial monitoring efforts, it was concluded that, under the conditions of our use, the long-path FT-IR could not compete with gas chromatographic techniques for the measurement of halocarbon species in terms of sensitivity and economy in generating high-volume data.

B. Second Year of Study

Due to scheduled University construction at the initial site of the FT-IR facility, it became necessary to move the instrumentation in early 1977 to a ground location adjacent to the SAPRC laboratory. At this new location, the 36 cm diameter air sample intake was raised to approximately 7 m above ground for clear reception of air masses from the west.

The second summer of the study program was characterized by a much higher incidence of smog episodes than was experienced in Riverside during the first year (1976). More definitive spectroscopic data for nitric acid and formaldehyde were obtained and the time-concentration behavior of these and the other pollutants observed were characterized for smog episodes in the eastern end of the South Coast Air Basin. The quantitative data thus obtained during the 1977 smog season are more extensive and well-defined than the data from the previous spectroscopic studies made by ourselves in 1976 (61) and by Hanst and co-workers (9) in 1973. The results of 5-8 hour monitoring periods for 10 episode days in July-October 1977 are reported in Tables A-2 to A-11 of Appendix A. The supplemental data on NO, NO_2, CO and nonmethane hydrocarbons (NMHC) reported in the data tabulations were derived from measurements by instrumentation in the adjacent California Air Resources Board's mobile laboratory which was also operated by SAPRC personnel.

Examples of spectra illustrating more definitive detection of HCHO and HNO_3 during the 1977 study are presented in Figures 9 and 10. The much improved signal-to-noise ratio attained in these spectra (compared with Figures 4 and 5) reflected the improvements made in our operating procedures as well as the higher pollutant concentrations found in the 1977 episodes.

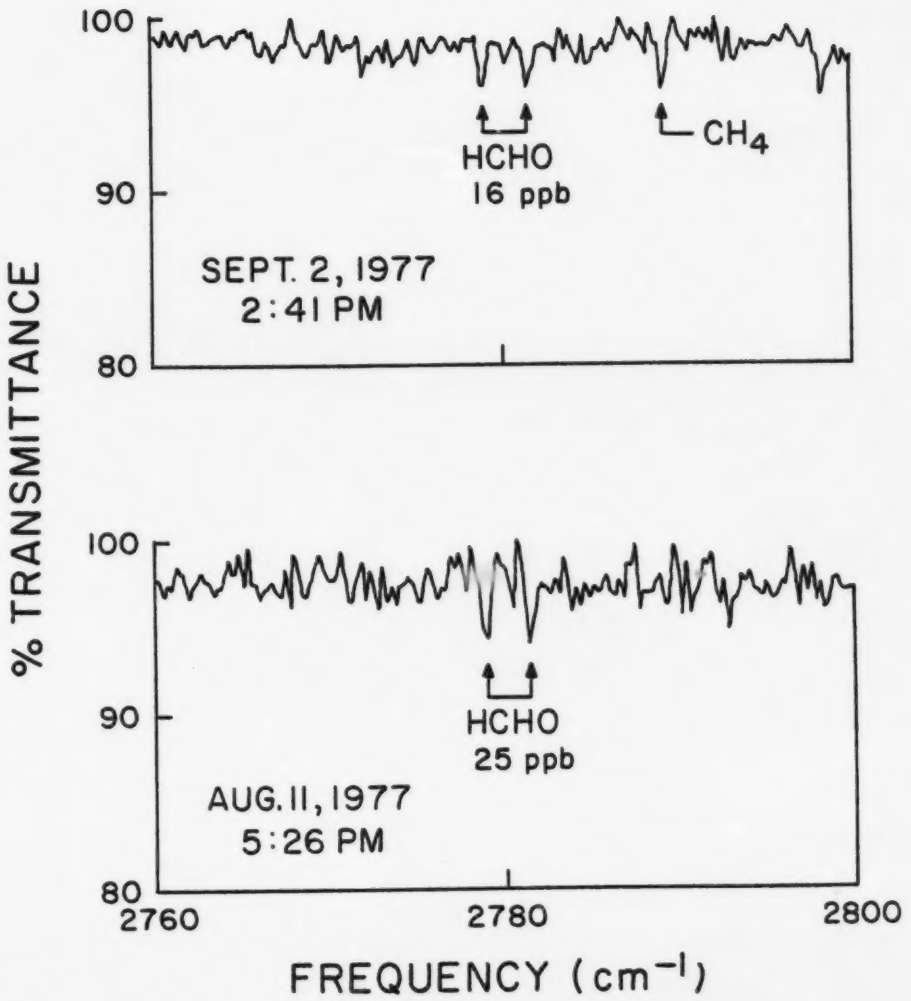

Figure 9. Riverside ambient air spectra at 0.5 cm^{-1} spectral resolution and 900 m pathlength with InSb detector.

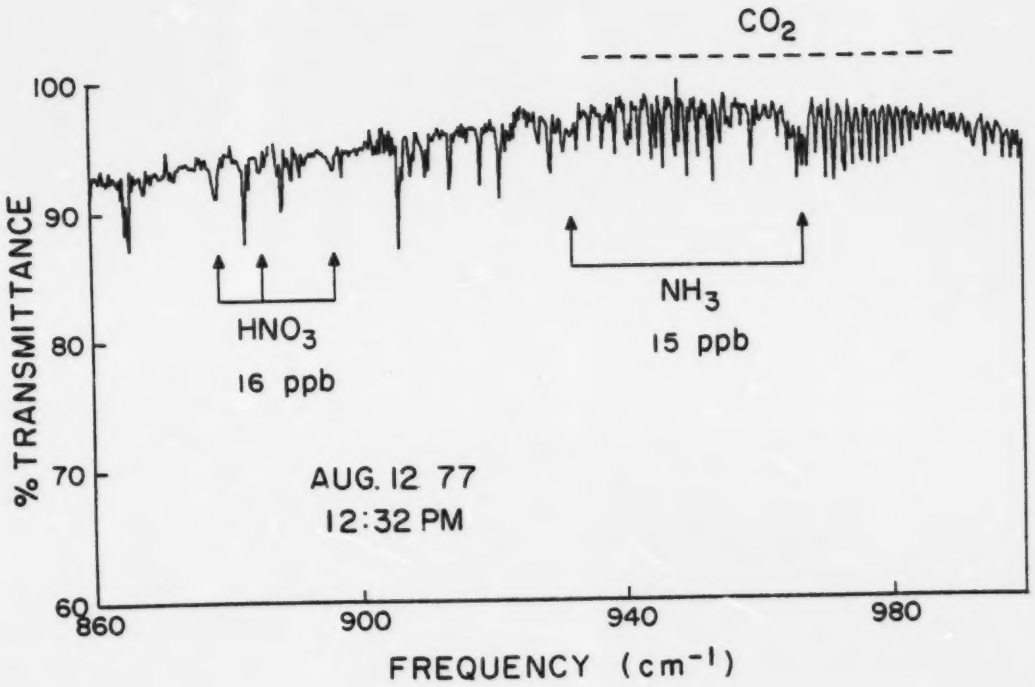

Figure 10. Riverside ambient air spectrum (August 12, 1977 at 12:32 p.m.) at 0.5 cm^{-1} spectral resolution and 900 m pathlength with HgCdTe detector.

The maximum concentrations of O_3, PAN, NH_3, HCOOH and HCHO observed during the 10 episode days reported here are given in Table 2. Figure 11 depicts the time-concentration profiles of the pollutants in the episode of October 14, 1977.

TABLE 2. MAXIMUM POLLUTANT CONCENTRATIONS (ppb) MEASURED IN RIVERSIDE AIR IN 1977

Date	O_3	PAN	NH_3	HNO_3	HCOOH	HCHO
Jul. 21	264	11	41	12	5	20
25	291	10	47	20	4	19
Aug. 10	234	10	40	*	8	19
11	287	13	39	13	10	27
12	249	11	46	16	11	25
Oct. 3	241	10	57	13	8	29
4	195	10	37	15	8	25
11	242	18	132	12	9	38
14	260	17	102	9	13	36
17	240	14	81	11	11	38

*Below detection limit.

The time-concentration behavior of HNO_3 is best treated in conjunction with the observed NH_3 concentration, since the earlier suggestion that the interaction of these two species is primarily responsible for the uniquely high levels of nitrate aerosol in the Riverside area (62,63) is strongly supported by the data of the 1977 study. In general, the HNO_3 concentration was near or below detection limit when high NH_3 concentrations were present; peak HNO_3 concentrations which coincided with the O_3 maxima were observed most clearly when the NH_3 levels were low. On several occasions NH_3 concentrations rose rapidly to well-defined peaks (see Figure 11) which preceeded the O_3 maxima, suggesting that NH_3 is being incorporated into the leading edge of the polluted air mass from agricultural sources upwind of Riverside. NH_3 concentrations as high as 132 ppb were measured by our instrument.

The 1977 FT-IR study in Riverside contained a significant body of data on the simultaneous concentrations of NH_3 and HNO_3 which were measured at short integration times. These data are precisely those which

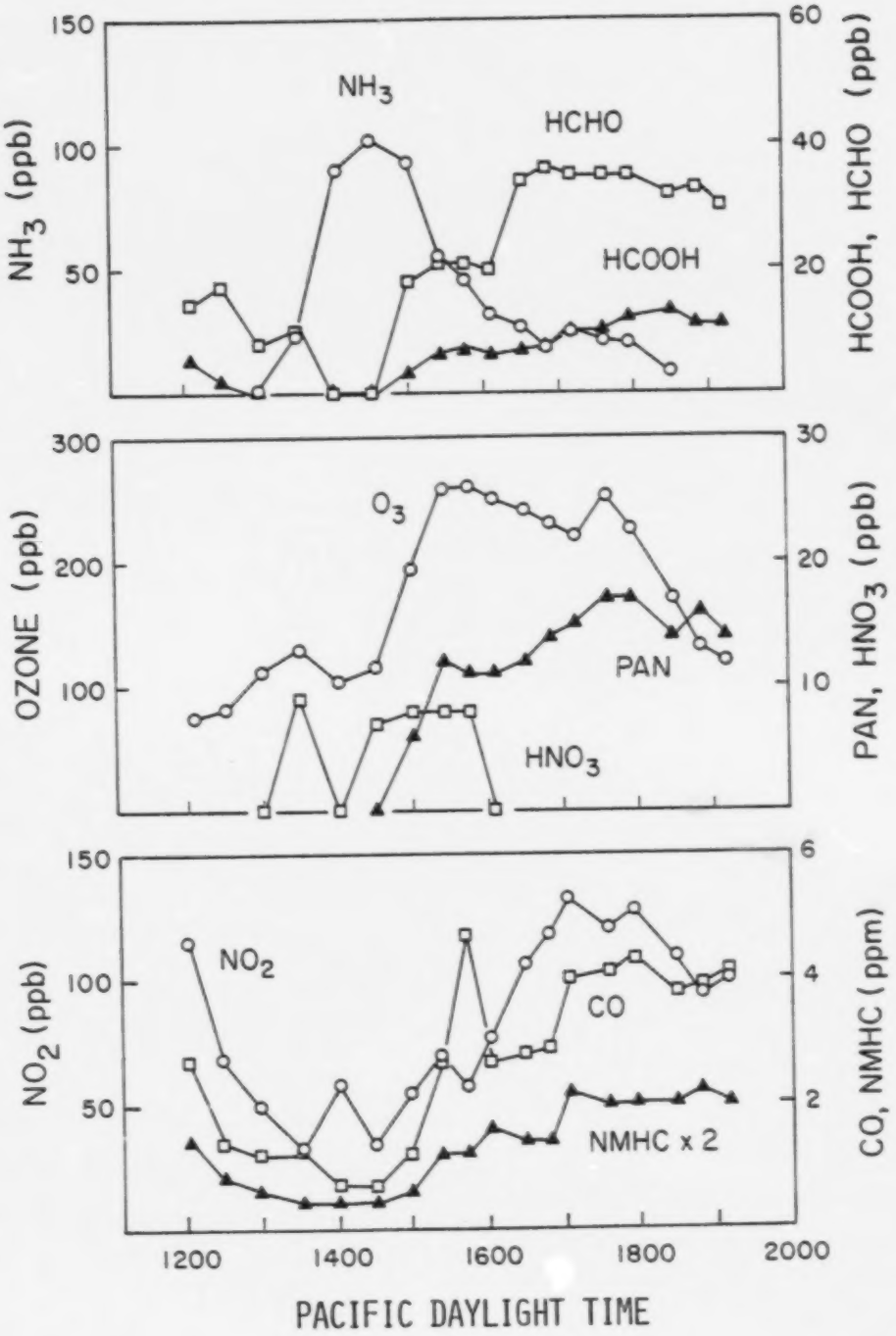

Figure 11. Time-concentration profiles obtained from 900 m pathlength FT-IR spectra of Riverside ambient air on October 14, 1977.

are needed to investigate the role that the precursors NH_3 and HNO_3 play in the formation of ammonium nitrate in the atmosphere and on sample-collection filters. Figure 12 shows the distribution of simultaneous NH_3 and HNO_3 concentrations derived from the episode days reported here and from short-period measurements on additional days. The relationship between NH_3-HNO_3 concentration products and temperature is plotted in Figure 13. Supplemental data from 24-hour filter collections provided information on the general levels of particulate NH_4NO_3. Analysis of these data supports the hypothesis that particulate NH_4NO_3 is in equilibrium with its gas phase precursors, NH_3 and HNO_3, and suggests that the ammonium nitrate equilibrium constant derived from published thermochemical data (Table 3) gives a reasonable upper limit for the concentration product of gas-phase NH_3 and HNO_3 in the atmosphere. A detailed discussion of these results is given in a recent publication (67).

In addition to the ambient air measurements, the long-path cell was employed in 1977 as an "outdoor smog chamber" in an investigation of the atmospheric reactions of alkyl-substituted amines (with NO_x). During this work the "unknown product" reported by Hanst et al. (68) as resulting from irradiation of the dimethylnitrosamine initially formed in amine/NO_x photooxidations was identified as dimethylnitramine $(CH_3)_2NNO_2$. Dimethyl- and diethylnitramine were shown to be the major gas-phase products, and the infrared spectrum obtained for diethylnitramine appears to be the first reported gas-phase spectrum for this compound (69).

C. Third Year of Study

In the summer of 1978, the FT-IR facility was moved from the UC Riverside campus to Claremont, California, and was installed on the roof of the Jacobs Science Center of Harvey Mudd College. Although moderate pollution episodes were recorded for various days during the summer months, this report focuses on the week of October 9-13, 1978 during which extended periods of air monitoring were carried out, including data collection for a continous 38-hour period for the more severe smog episodes on October 12 and 13. This week was characterized by a monotonic rise in the daily peak O_3 readings from 0.16 ppm on Monday, October 9, to 0.45 ppm on Friday,

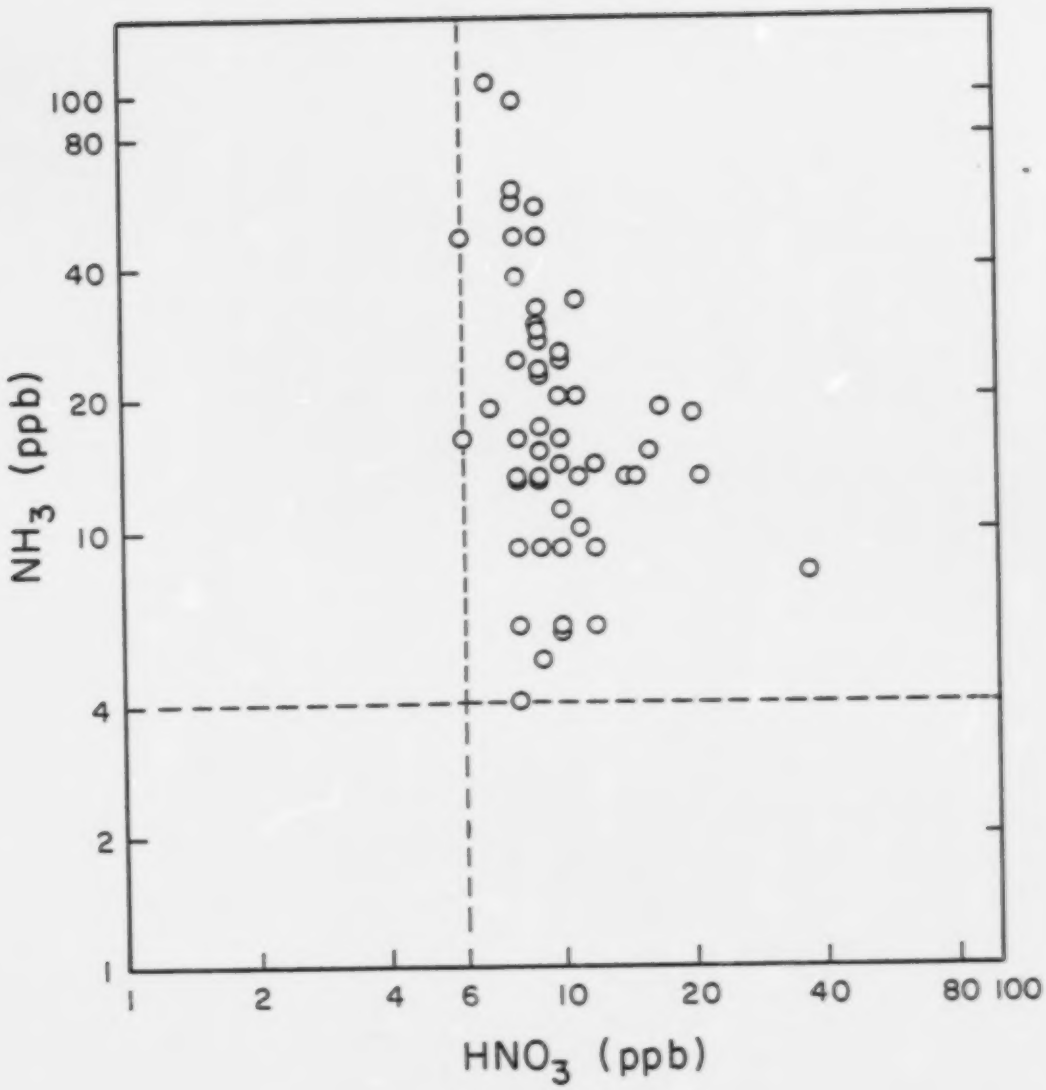

Figure 12. Distribution of simultaneous observations of ammonia and nitric acid concentrations: (---) detection threshold.

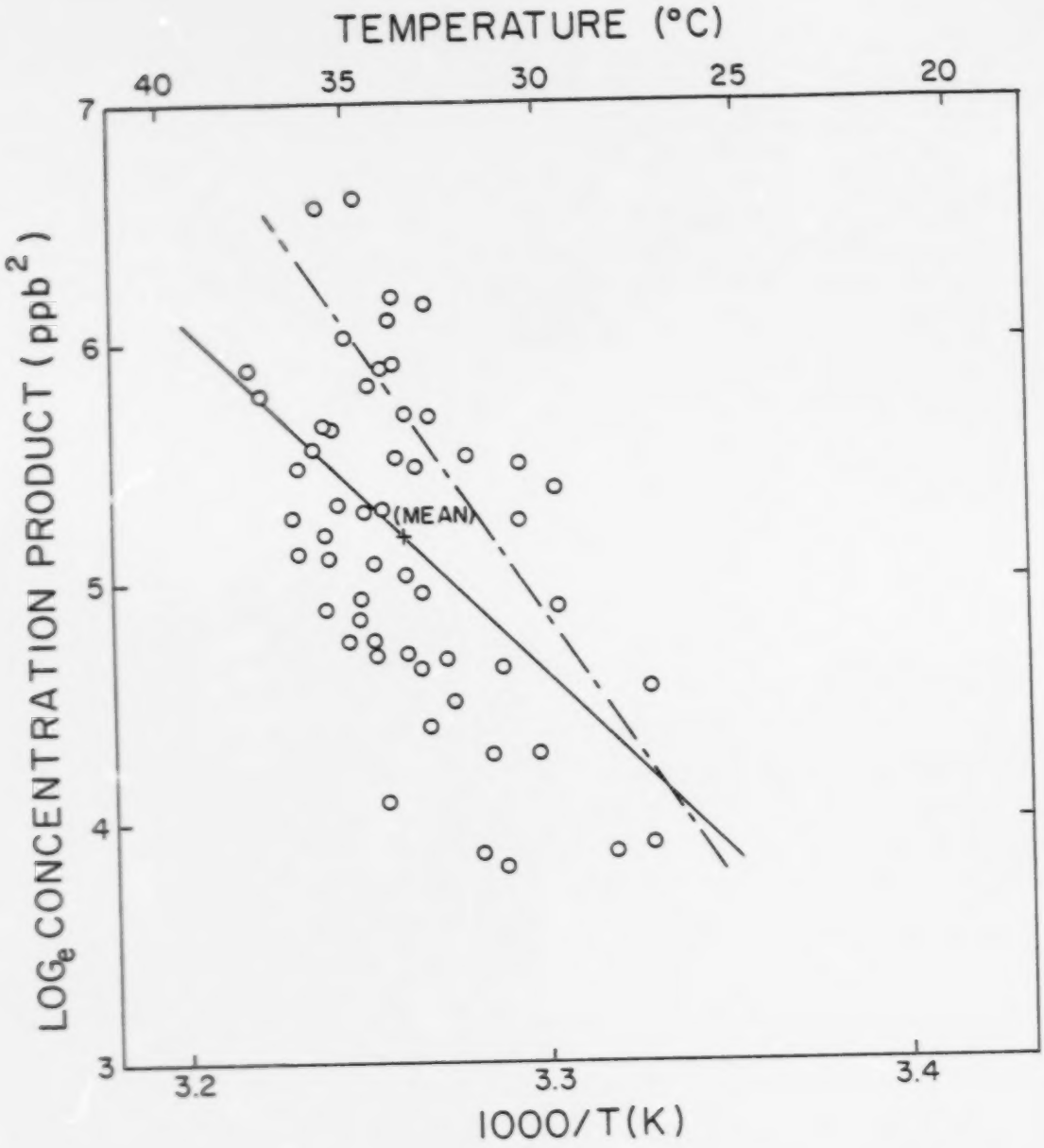

Figure 13. Logarithm of the NH_3-HNO_3 concentration product vs. the reciprocal absolute ambient temperature: (—) regression line calculated from unweighted experimental data (54 observations); (– – –) regression line calculated from thermodynamic data.

TABLE 3. THERMODYNAMIC DATA FOR THE NH_4NO_3 EQUILIBRIUM AT 306.6 K*

	Derived from Experimental Data	Calculated from Thermodynamic Data
Free-energy change kcal/mol	22.08 (± 0.12)	21.78
Enthalpy change kcal/mol	30 (± 12)	43.79

*Average of all temperatures in these experiments.

The temperature and free-energy change are the means of the 54 observations. Enthalpy is calculated from the slope of the unweighed regression line. The uncertainties in parentheses are 95% confidence intervals.

Calculated at 306.6 K from heat of formation data given by JANAF Tables (64) and by Wagman et al. (65) using gas heat capacities from Benson (66) and solid heat capacities from Wagman et al. (19). The small heat of transition contribution for NH_4NO_3 at 305.4 K was included (ΔH = 0.410 kcal/mol).

October 13, and represents a "classic" stagnant air episode with pollutant "carryover" and progressively increasing oxidant levels.

The measured concentrations of O_3, PAN, HNO_3, HCOOH and HCHO as a function of time are presented in Tables A-10 to A-14. The daily maximum concentrations are summarized in Table 4. Results of measurements for a continuous 38-hour period during October 12 and 13, 1978 are graphically presented in Figure 14. Supplemental data on NO_x concentrations were also obtained on October 13 (Table A-14) with a TECO chemiluminescent analyzer. The NO_2 concentrations given in Table A-14 have been corrected for interferences (21,22) due to PAN and HNO_3.

Formaldehyde. In a recent article, Altshuller (70) singled out HCHO as the most significant eye irritant in photochemical smog. Peak concentrations as high as 160 ppb and an average level of 40 ppb were reported (14,71) in 1960 and 1961 for downtown Los Angeles. These earlier studies employed colorimetric methods with chromotropic acid reagents. More recent wet chemical measurements (72) of formaldehyde concentrations

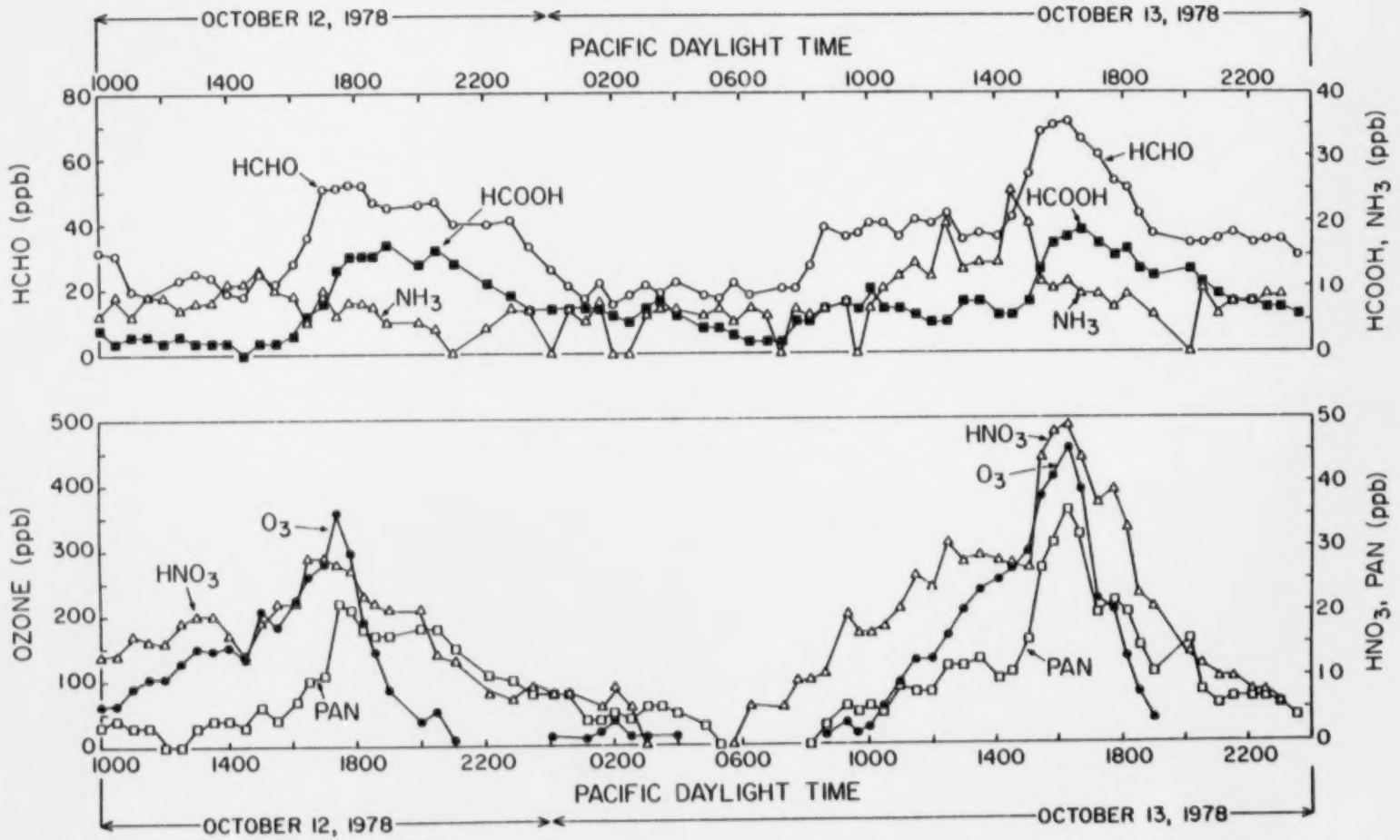

Figure 14. Concentrations of ozone and other pollutants in photochemical smog measured at Claremont, California, October 1978.

TABLE 4. DAILY MAXIMUM CONCENTRATIONS (ppb) OBSERVED IN CLAREMONT, CA BY KILOMETER PATHLENGTH FT-IR SPECTROSCOPY

Date	O_3	PAN	NH_3	HNO_3	HCOOH	HCHO
October 9	163	6	11	18	5	23
10	227	14	23	28	5	30
11	280	13	13	30	7	31
12	360	22	13	29	17	52
13	454	37	25	49	19	71

in the atmospheres of four New Jersey cities have been made by the New Jersey Department of Environmental Protection (73). They reported peak formaldehyde concentrations at the four sites in the range 14-20 ppb and also provided diurnal concentration data for two of the sites.

In the present study, morning HCHO concentrations in Claremont were found to be in the range of 20-40 ppb. A slight decrease in these concentrations occurred around the noon hours and prior to the peak O_3 readings. During the moderate episodes on Monday to Wednesday, October 9-11, the HCHO levels did not significantly rise above the morning HCHO concentrations. However, well-defined HCHO peaks corresponding to O_3 maxima were observed (Figure 14, Tables A-13 and A-14) during the more severe episodes of Thursday and Friday, October 12 and 13, with HCHO reaching a peak concentration of 71 ppb at about 1600 hr on the 13th. The observations in Claremont suggest that the high levels of HCHO formed in the early studies (14,71) may indeed be approached under conditions of intense photochemical air pollution. Figure 14 also shows the persistence of ~20 ppb of HCHO during the night, an important observation in modeling the role of formaldehyde as an early morning catalyst for smog formation. Representative spectra showing the buildup of HCHO on October 13 are given in Figure 15.

Formic Acid. HCOOH levels were generally low, typically less than 10 ppb even during moderate episodes (Tables A-10 and A-12). This agrees with the majority of our measurements in 1977 at Riverside (Tables A2-9; ref. 61). Highest concentrations at Claremont were recorded during the episodes on Thursday and Friday (October 12 and 13) with a maximum of 19 ppb. A peak HCOOH concentration of 19 ppb was also recorded by Hanst et al. (9) in their FT-IR study of the intense episode which occurred in

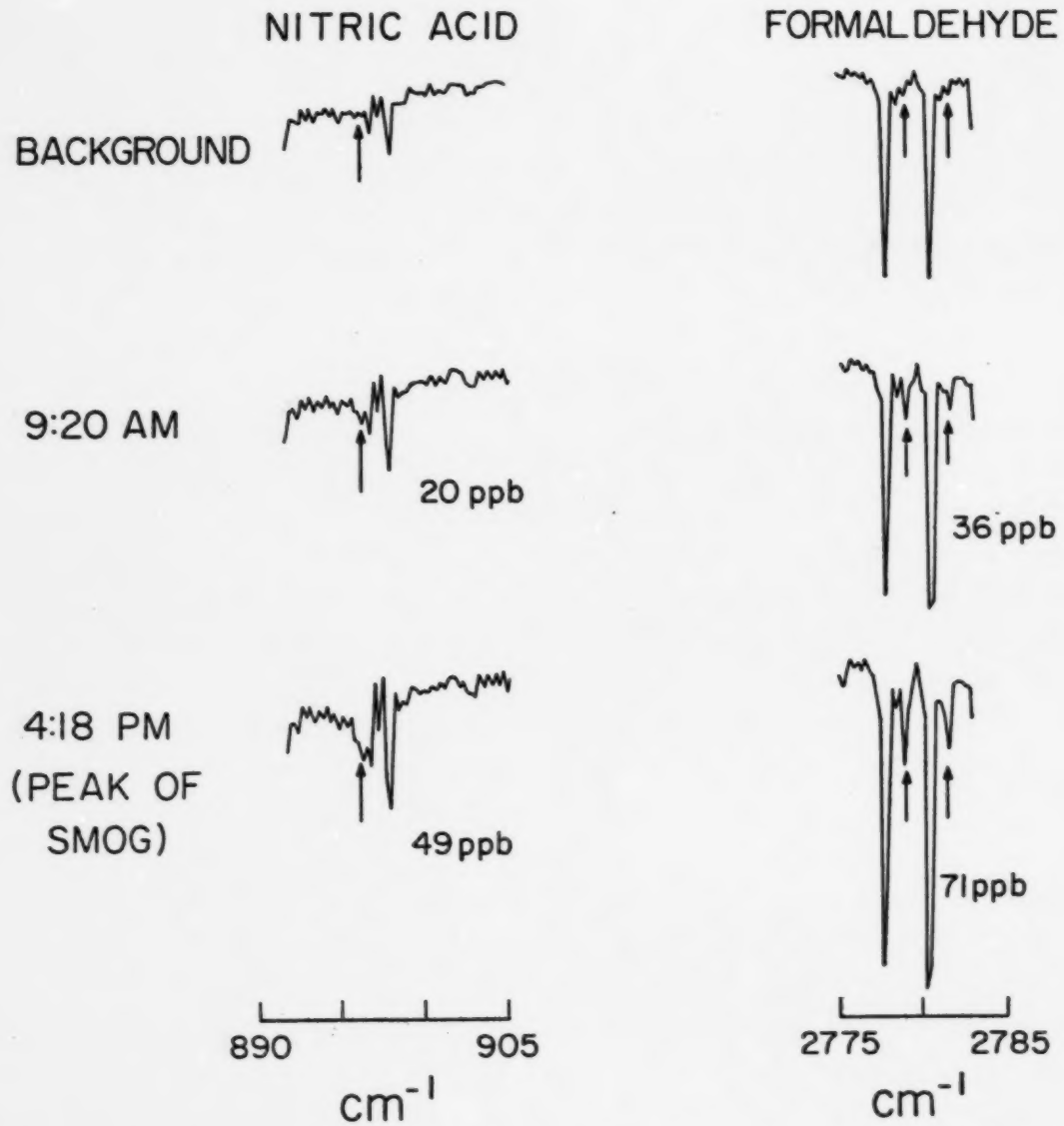

Figure 15. Single-beam spectra showing the concentration levels of nitric acid (HNO_3) and formaldehyde (HCHO) during the severe smog episode of October, 1978, Claremont, California.

Pasadena on July 25, 1973. However, the HCOOH data of Hanst and co-workers (9) must be divided by 3.8 to be compatible with our recent absorptivity measurement (Table 1) of the 1105 cm^{-1} Q-branch. As indicated in Figure 14, the HCOOH concentration peaks on October 12 and 13 occurred approximately one hour after the HCHO maxima.

Nitric Acid. Although we had accumulated substantial HNO_3 data during the 1977 study in Riverside (Tables A-2 to A-9; ref. 62), these profiles consisted only of upper limits during many periods (i.e., concentrations were below the detection limit) and thus a detailed characterization of HNO_3 concentrations as a function of photochemical activity was not possible. The simultaneous occurrence of high NH_3 concentrations (i.e. up to 130 ppb) during these periods has been strongly suggested (62,63) as a cause of HNO_3 depletion and NH_4NO_3 aerosol formation. The Claremont site allowed the study of ambient levels of HNO_3 at prevailing low NH_3 concentrations which are more typical of those occurring at other locations in the South Coast Air Basin.

Figure 14 shows that the rise in HNO_3 concentration is strongly coincident with the increase in oxidant levels (e.g., O_3 and PAN). This behavior is also characteristic of the more moderate episodes on October 9 to October 11 (Tables A-10 to A-12). The highest HNO_3 concentration measured was 49 ppb which coincided with the O_3 concentration of 454 ppb recorded on October 13. The growth of the HNO_3 absorption during the episode is shown in Figure 15. Our measurements compare favorably with HNO_3 concentrations measured by Spicer (11) in 1973 at West Covina in which one-hour maxima of 40 ppb HNO_3 at 271 ppb O_3 and 34 ppb HNO_3 at 213 ppb O_3 were recorded.

The important reactions for the formation of HNO_3 are

$$N_2O_5 + H_2O \rightarrow 2\ HNO_3 \text{ (heterogeneous)}$$

and

$$OH + NO_2 + M \rightarrow HNO_3 + M$$

Although the first reaction has been postulated as the predominant pathway for HNO_3 formation, the second reaction may account for most of the HNO_3 formed early in the day since N_2O_5 is formed primarily from reactions initiated by O_3. Using a rate constant (3,74,75) of $\simeq 1.5 \times 10^4$ ppm^{-1} min^{-1}

for the second reaction, and taking typical OH radical and NO_2 concentrations (3,75) of 10^{-7} ppm and of 0.1 ppm, respectively, calculations indicate that 15 ppb of HNO_3 could be generated in a period of 100 minutes in the absence of a rapid removal process. Indeed, mid-morning (e.g., ~10 a.m.) concentrations of HNO_3 in Claremont during the week of October 9-13, 1978 were typically in the range of 10-15 ppb.

Ammonia. NH_3 has been assigned a prominent role in the formation and neutralization of sulfate and nitrate aerosols. Particulate sulfates and nitrates in the inland areas of the South Coast Air Basin (SCAB) have been shown (63,76-78) to exist mainly in the form of ammonium salts and their spatial distribution in the SCAB has been strongly correlated with prevailing local NH_3 concentrations.

The average NH_3 concentration measured in Claremont during the week of October 9-13 was ~8 ppb. An examination of our data obtained during the months of July and August, 1978, also indicated that the NH_3 level in Claremont is generally less than 10 ppb. Recent preliminary measurements by a filter collection method (79) employing oxalic acid-coated filters gave a similar range (1-10 ppb) for NH_3 concentrations in other locations in the South Coast Air Basin outside of the Riverside-San Bernardino area. The NH_3 concentrations measured by FT-IR spectroscopy in Claremont were approximately five times lower than those found in Riverside during our 1976 and 1977 studies. Incorporation of high NH_3 levels into the polluted air mass from primary sources (i.e., feedlots) in the Chino and Ontario area was evident in the Riverside data (Tables A-2 to A-9; ref. 61). Claremont is approximately seven miles northwest of the Chino-Ontario area and although air mass transport is mainly eastward toward the Riverside-San Bernardino area, an occasional increase in NH_3 concentrations up to ~25 ppb (see Figure 13) may be attributed to diffusion from this primary source.

In summary, the 1978 air monitoring study in Claremont has been our most successful attempt at characterizing the levels of trace pollutants in the atmosphere by long-path FT-IR spectroscopy. The sampling location is more representative of other sites in the California South Coast Air Basin and the data gathered encompass smog episodes of progressively increasing

intensity and duration. The data reported here are the most comprehensive simultaneous measurements of HNO_3, HCHO, HCOOH, NH_3, PAN and O_3 in photochemical smog which have been published to date.

D. Fourth Year of Study

1. Field Study to Intercompare Methods for Measurement of Nitric Acid and Aerosol Nitrate in Ambient Air

The discovery of artifactual errors in the widely accepted method for measuring nitrates in the atmosphere by sample collection on fiberglass filters has raised serious questions concerning the validity and utility of the bulk of earlier data on aerosol nitrate levels. The recognition of this problem provided impetus for researchers to develop new, more sensitive and selective techniques for the measurement of both gaseous and particulate nitrates (80). Many of the problems associated with nitrate measurements were addressed formally during a workshop held at the U.S. Environmental Protection Agency in October 1978. One outcome of that meeting was the development of a plan to conduct a field experiment that would bring together appropriate research groups to intercompare methods for nitrate measurements.

The major aim of the study was to perform aerosol nitrate measurements simultaneously with measurements of gaseous nitric acid and other appropriate chemical species and physical parameters in order to acquire data which would be useful in identifying the causes of artifact (both positive and negative) and to quantify these errors. Accurate determinations of gas phase nitric acid concentrations was considered to be crucial to the interpretation of the results of this study. It was recognized at that time that the long-path FT-IR technique could serve as a standard for nitric acid determination since the measurements involve an in situ, nondestructive technique and identification is made unambiguously by recognition of characteristic spectral features.

Field Study Protocol. During the period August 27-September 3, 1979, a field measurement study was conducted at the site of our long-path FT-IR facility in Claremont, California. The participants in the study included research groups from the U.S. Environmental Protection Agency (EPA), Battelle (Columbus Laboratories), Brookhaven National Laboratory

(BNL), National Center for Atmospheric Research (NCAR), Oregon Graduate Center, University of Michigan, Harvey-Mudd College, and UCR-SAPRC.

A summary of the nitric acid and particulate nitrate methods employed in the study is given in Table 5. Detailed descriptions of the individual methods are contained in the "Handbook on Measurement of Atmospheric Nitrates" (80), a publication which resulted from the workshop held in October 1978. Table 6 shows the nitric acid and particulate nitrate sampling schedule which was followed during the field tests. The eight test days were divided into a total of 32 time blocks of 3-, 6-, and 12-hour duration. The FT-IR technique, utilized as a standard for nitric acid measurement, provided ~120 hours of monitoring representing no less than 220 real-time data points.

Ancillary measurements for other chemical species and physical parameters are summarized in Table 7. Reliable measurements of NH_3, a key species in this study, as well as PAN and HCHO were additionally provided by FT-IR monitoring. In the case of PAN, a GC instrument was set up by SAPRC and recorded concentrations at 15-minute intervals; the GC calibration was validated by comparison with the corresponding FT-IR data obtained at several times during the study.

Results of the Intercomparison Among Nitric Acid Measurement Methods. The period during which the field experiments were conducted was characterized by very low to moderate pollution days. HNO_3 concentrations were near or below detection limit for a significant portion of the total measurement period. The detailed results of the FT-IR monitoring are given in Table A-15 of Appendix A. Supplemental data on O_3 from a Dasibi instrument are also included in Table A-15, while the GC results for PAN concentrations are given in Table A-16.

The results of the eight-day field study in Claremont are summarized in a preliminary report (81) which was prepared by Battelle (the prime contractor of the collaboration study) for an informal symposium held at EPA-RTP Laboratories on May 20, 1980. Tables 5-7 were reproduced from the above report. Data for the nitric acid intercomparison are shown in Table 8 with the block-averaged HNO_3 concentrations expressed in micrograms per cubic meter ($\mu g\ m^{-3}$). The codes for the individual analytical methods are those which are given in Table 5. Table 8 differs from that presented in the

TABLE 5. METHODS FOR MEASUREMENT OF NITRIC ACID AND PARTICULATE NITRATE

Organization	Code	Sampling Method*	Nominal Sampling Rate	Analysis Method	Location of Experiment†	Data Obtained			
						HNO_3	Fine NO_3^-	Coarse NO_3^-	Total NO_3^-
Battelle	BAT/CHEM	1.2 μ Ghia nylon filter for HNO_3	1 ℓpm	Cont. chemiluminescent analyzer	RP	X			
Battelle	BAT/LVF	47 mm 1 μ Zefluor/1.2 μ Ghia nylon filters	12 ℓpm	Ion chromatography	OR	X			X
Battelle	BAT/HVFQ	8" x 10" Pallflex 2500 QAST quartz filter	1.14 m^3/min	Ion chromatography	OR				X
Battelle	BAT/HVFG	8" x 10" S&S (NASN) glass filter	1.14 m^3/min	Ion chromatography	OR				X
Brookhaven	BNL/LVF	47 mm Fluoropore/NaCl impreg. cellulose filters	10-20 ℓpm	Technicon analyzer (colorimetric)	OR	X			X
Brookhaven	BNL/DDE	Heated $NaCO_3$ denuder tube/ 47 mm 0.5 μ Fluoropore filter/ NaCl impreg. cellulose	20 ℓpm	Technicon analyzer (colorimetric)	OR	X			X
Brookhaven	BNL/HVF	5" treated quartz/NaCl impreg. cellulose	0.57 m^3/min	Technicon analyzer (colorimetric)	OR	X			X
U.S. EPA	EPA/NTR	47 mm Ghia Teflon filter/nylon fiber trap	1 ℓpm	Gas chromatography (EC)	OR	X			
U.S. EPA	EPA/NTML	47 mm Ghia Teflon filter/nylon fiber trap	1 ℓpm	Gas chromatography (EC)	ML	X			
U.S. EPA	EPA/DDE1	DDE System #1, Parallel samplers: 1) MgO Denuder tube/47 mm Ghia 1 μ Teflon filter/nylon fiber trap	1-3 ℓpm	Nylon trap - Gas chromatography (EC)					
		2) 47 mm 1 μ Ghia Teflon filter/ nylont fiber trap	1-3 ℓpm	Teflon filter - Ion chromatography	OR&RP	X			X
U.S. EPA	EPA/TFDDE1	DDE System #1 47 mm 1 μ Ghia Teflon filter/ nylon fiber trap	1-3 ℓpm	Nylon trap - Gas chromatography (EC) Teflon filter - Ion chromatography	OR&RP	X			X
U.S. EPA	EPA/DDE2	DDE System #2, Parallel samplers: 1) MgO Denuder tube/47 mm Ghia 1 μ Teflon filter/nylon fiber trap	1-3 ℓpm	Nylon trap - Gas chromatography (EC) Teflon filter - Ion chromatography	OR&RP	X			X
		2) 47 mm 1 μ Ghia Teflon filter/ nylon fiber trap	1-3 ℓpm	Nylon trap - Gas chromatography (EC) Teflon filter - Ion chromatography	OR&RP	X			X
U.S. EPA	EPA/TFDDE2	DDE System #2 47 mm 1 μ Ghia Teflon filter/ nylon fiber trap	1-3 ℓpm	Nylon trap - Gas chromatography (EC) Teflon filter - Ion chromatography	OR&RP	X			X
U.S. EPA	EPA/BDSTA	Beckman dichotomous sampler, 1 μ Ghia Teflon filters	16.7 ℓpm†	Technicon analyzer (Cd Red)	OR		X	X	X
U.S. EPA	EPA/LBLDSTA	Lawrence Berkeley Laboratory dichotomous sampler, 1 μ Ghia Teflon filters	50 ℓpm†	Technicon analyzer (Cd Red)	ML		X	X	X
U.S. EPA	EPA/LBLDSIC	LBL dichotomous sampler (same samples as above)	50 ℓpm†	Ion chromatography	ML		X	X	X
NCAR	NCAR/LVF	90 mm, 1 μ Zefluor/1 μ Ghia nylon	20 ℓpm	Technicon analyzer	OR	X			X
U. California (Riverside)	UCR/IR		Static	FTIR, 1 km pathlength	OR	X			
U. Michigan	UM/CHEM	Nylon wool trap for HNO_3		Cont. chemiluminescent analyzer	ML	X			

*See Ref. 81 for more detailed description of the individual methods.

†RP - Sample taken from manifold into roof penthouse

OR - Open roof

ML - Mobile laboratory in parking area.

†Total flow rate; flow distribution ~10 percent coarse/~90 percent time.

TABLE 6. NITRIC ACID AND PARTICULATE NITRATE SAMPLING SCHEDULE

Sampling Block No.	Sampling Intervals During Test Days (hrs PDT)							
	Day 1 8/27/79	Day 2 8/28/79	Day 3 8/29/79	Day 4 8/30/79	Day 5 8/31/79	Day 6 9/1/79	Day 7 9/2/79	Day 8 9/3/79
1	0600-1800*	0000-1200*	0000-0600	0000-0300	0000-0300	0000-0600	0000-0600*	0000-0600
2	1800-2400*	1200-1800*	0600-0900†	0300-0900	0300-0900	0600-1200*	0600-0900†	0600-1200*
3	-	1800-2400	0900-1500*	0900-1500*	0900-1200†	1200-1500†	0900-1200†	1200-1500†
4	-	-	1500-1800†	1500-1800†	1200-1800*	1500-1800†	1200-2400*	-
5	-	-	1800-2400	1800-2400	1800-2400*	1800-2400*	-	-

*IR measurement made every 30 minutes

†IR measurement made every 15 minutes

Breakdown of Sampling Blocks

Total Blocks	Blocks with IR Measurements
11-3 hr blocks	9-3 hr blocks
18-6 hr blocks	10-6 hr blocks
3-12 hr blocks	3-12 hr blocks

TABLE 7. ANCILLARY MEASUREMENTS FOR THE NITRIC ACID/PARTICULATE NITRATE FIELD STUDY

Parameter	Organization
NO	EPA University of Michigan
NO_2	EPA University of Michigan
PAN	UCR-SAPRC
NH_3	EPA UCR-SAPRC
NH_4^+	EPA Battelle
NO_2^-	EPA Battelle
O_3	EPA UCR-SAPRC
CO	EPA
Total sulfur	EPA
Continuous sulfate	Brookhaven Oregon Graduate Center
HCl	NCAR
H_2O_2	Harvey Mudd College
HCHO	Harvey Mudd College UCR-SAPRC
Aerosol size distribution	EPA
Light scattering coefficient	EPA
$SO_4^=$	Brookhaven Battelle EPA
Aerosol acidity	Brookhaven Battelle EPA
UV intensity	EPA
Temperature and humidity	Battelle UCR-SAPRC
Wind Speed and direction	Battelle

preliminary report (81) in that several additional valid data entries were included from the long-path FT-IR measurements (UCR/IR). These additional data points are averages of the upper and lower limit HNO_3 concentrations for individual blocks which had measurements above and below the detection limit. As an example, for a 3-hour test block containing 12 measurements with 5 points below detection limit, the 7 measurable values were added and divided by 12 to obtain the lower limit estimate for the block; the upper limit was calculated by adding 5 x 7 ppb (7 ppb being the next highest detectable concentration) to the total of the 7 measured values and the resulting figure divided by 12.

Of the 22 measurement blocks which called for FT-IR measurements, 6 were indeterminate due to levels of HNO_3 which were predominantly below detection limit (less than 6 ppb or 15 $\mu g\ m^{-3}$) and 4 were incomplete owing to instrument malfunctions. Nevertheless, the 12 block-averaged data points reported in Table 8 are sufficient to establish a comparison with the results of the other methods for concentration levels of HNO_3 which are within the detection sensitivity of the FT-IR instrument.

The statistics for the regression fits for nitric acid using the FT-IR data as a standard are summarized in Table 9. Methods which yielded very few data points that corresponded with the FT-IR measurements (Table 8) are not treated. Likewise, the results of the UM/CHEM method, which suffered from a leak in the vacuum system of the instrument throughout the field study, was also excluded from the comparison. The intercept of the regression line measures the constant bias of a method while the slope measures the proportional bias. The standard errors for intercept and slope are given as indications of whether intercept = 0 and slope = 1 are contained in the regression fit for each method. The mean square error is indicative of the precision of the method. Regression fits of the FT-IR data with the HNO_3 concentrations determined by four of the other measurement methods (BAT/CHEM, BUL/HVF, EPA/NTR and NCAR/LVF) are plotted in Figures 16 and 17.

Table 9 shows that a number of the methods employed for HNO_3 measurement compare favorably with the long-path FT-IR technique under actual field conditions. Thus, there is probably no truly significant differences, in terms of relative accuracy, among the results from the BAT/CHEM, BAT/LVF, BNL/LVF, and BNL/HVF methods. The relatively large errors in the intercept

TABLE 8. RESULTS OF NITRIC ACID MEASUREMENTS

Day	Block	Nitric Acid Concentration, Micrograms/Cubic Meter												
		BAT/ CHEM	BAT/ LVF	BNL/ LVF	BNL/ HVF	BNL/ DDE	EPA/ NTR	EPA/ DDE1	EPA/ TFDDE1	EPA/ DDE2	EPA/ TFDDE2	NCAR/ LVF	UCR/ IR†	UM/ CHEM
1	1	26.8	40.0	13.2*	33.5	5.5*	42.9	15.0	30.7*	4.6*	33.6	41.4*	28.0	**
1	2	12.3	**	**	**	**	**	-3.6	6.6	2.2	3.9	**	-	4.6
2	1	8.1	10.1	4.3	7.5	6.5	4.4	9.9	8.4	.9	7.8	6.7	-	3.9
2	2	22.0	26.3	19.9	20.1	20.7	25.7	12.3	12.7	9.3	13.1	18.9	20.7	7.7
2	3	12.3	3.6	2.9	2.9	6.8	8.2	6.3	1.5	10.5	11.6	3.6		6.1
3	1	2.6	4.5	3.3	2.9	8.8	10.6	-.1	2.1	.1	4.8	4.5		4.8
3	2	3.4	**	2.5	1.2	1.1	10.0	8.1	1.5	***	***	3.7	-	3.5
3	3	12.9	13.6	14.1	10.5	13.1	8.7	***	***	***	***	14.2	14.5	6.5
3	4	14.4	19.1	8.5	11.2	7.2	12.4	***	***	***	***	15.4	10.5	8.8
3	5	5.8	6.9	6.6	4.7	9.6	7.8	.4	5.9	***	***	7.3		6.2
4	1	4.5	3.3	1.7	1.2	7.2	3.5	8.6	18.4	***	***	2.5		9.1
4	2	.8	1.9	2.6	1.3	4.7	1.8	***	***	***	***	1.7		6.2
4	3	15.2	24.6	15.1	17.5	12.7	16.9	-3.0*	-.4*	***	***	22.7	23.0	4.9
4	4	24.9	33.5	28.4	21.7	28.0	33.4	***	***	21.1	26.9	29.8	21.5	7.3
4	5	5.9	**	5.1	5.8	6.2	4.1	***	***	2.7	3.6	8.6		8.8
5	1	0	***	3.5	1.9	3.3	9.5	***	***	***	***	2.2		4.5
5	2	1.8	7.5	3.2	2.4	**	3.5	***	***	***	***	5.7		4.0
5	3	19.7	22.5	20.8	14.6	17.5	23.7	***	***	7.2	8.4	20.4	25.7	4.0
5	4	31.0	42.1	25.9	30.3	20.4	35.5	***	***	15.6	20.6	21.8	32.0	3.7
5	5	8.4	7.7	6.0	4.9	6.7	1.8	6.0	10.9	***	***	7.5	-	3.4
6	1	2.6	4.5	2.8	1.8	7.1	7.1	***	***	***	**	3.0		2.7
6	2	13.4	15.3	10.2	8.2	12.2	***	***	***	***	***	15.1	13.5	**
6	3	31.8*	32.0	20.6	21.2	13.4	***	11.7	16.0	15.9	18.7	20.7	--	***
6	4	25.8	59.8*	36.3	27.1	34.3	11.3	14.0	11.9	17.5	33.2	***	27.0	***
6	5	13.8	14.1	9.7	9.3	8.1	24.7	***	***	6.5	6.0	***	-	***
7	1	3.2	10.3	6.7	5.6	6.4	1.4	***	***	5.3	5.3	9.2	-	***
7	2	5.2	**	8.4	5.1	9.1	3.3	***	***	**	**	**	--	***
7	3	24.9	**	30.0	24.9	21.6	20.9	***	***	***	***	***	--	***
7	4	17.1	27.5	23.5	20.0	19.8	9.9	11.5	15.0	8.8	11.3	24.4	17.5	***
8	1	***	12.2	7.9	6.6	4.8	2.0	4.2	3.6	5.8	5.1	7.8		7.6
8	2	17.9	21.8	22.8	19.5	17.1	**	***	***	10.3	15.9	2.4*	--	8.3
8	3	36.8	45.6	48.9	33.1	45.1	**	***	***	24.9	36.3	**	38.0	6.6

†Blank means no scheduled measurements

*Statistical outlier

**Removed for experimental reasons

***Data not reported

- Block average indeterminate due to high proportion of HNO_3 concentrations below FT-IR detection limit

-- Instrument malfunction

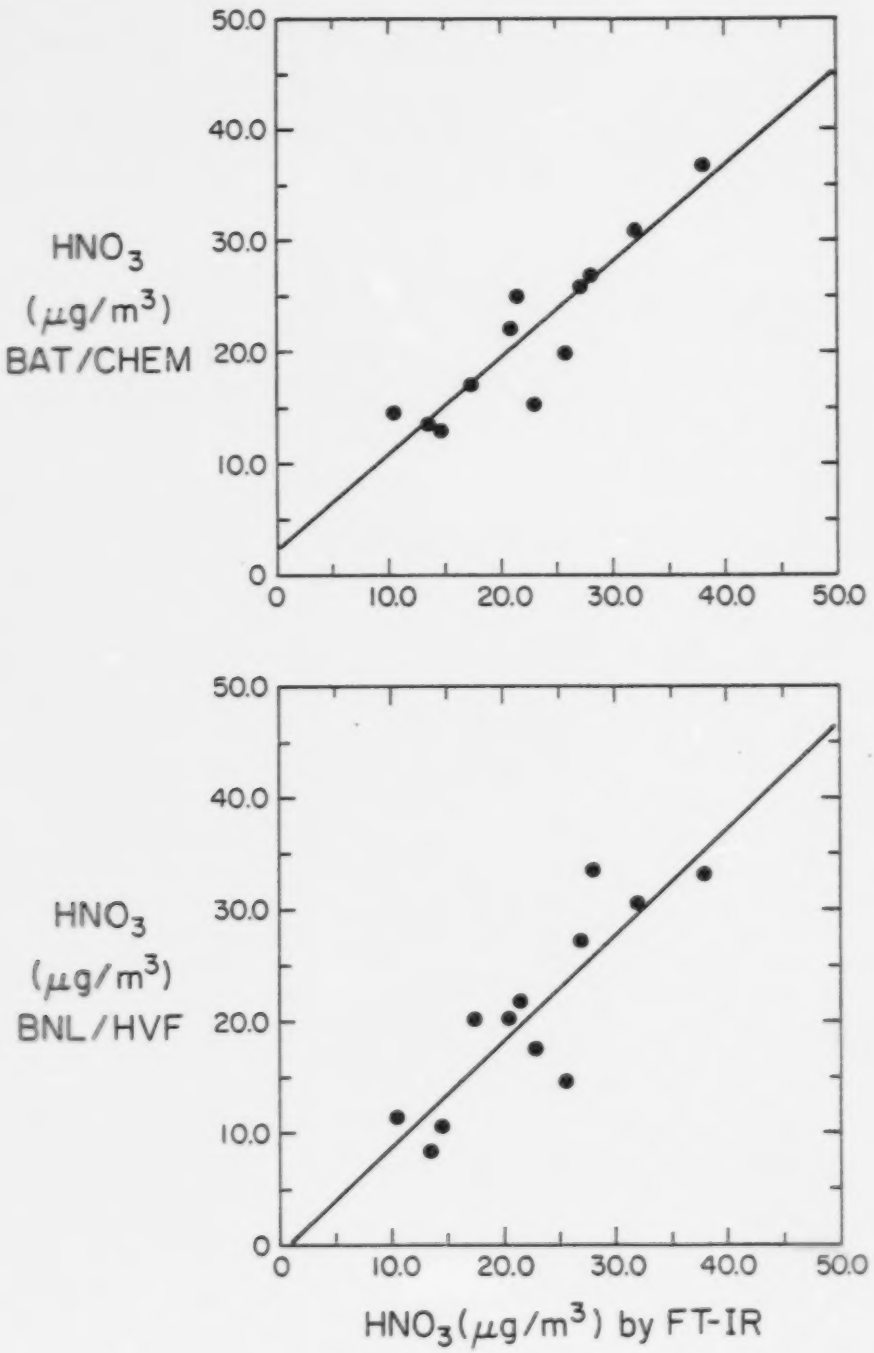

Figure 16. Regression fits of the FT-IR HNO_3 data with those obtained by the BAT/CHEM and BNL/HVF methods.

SAPRC 1430a

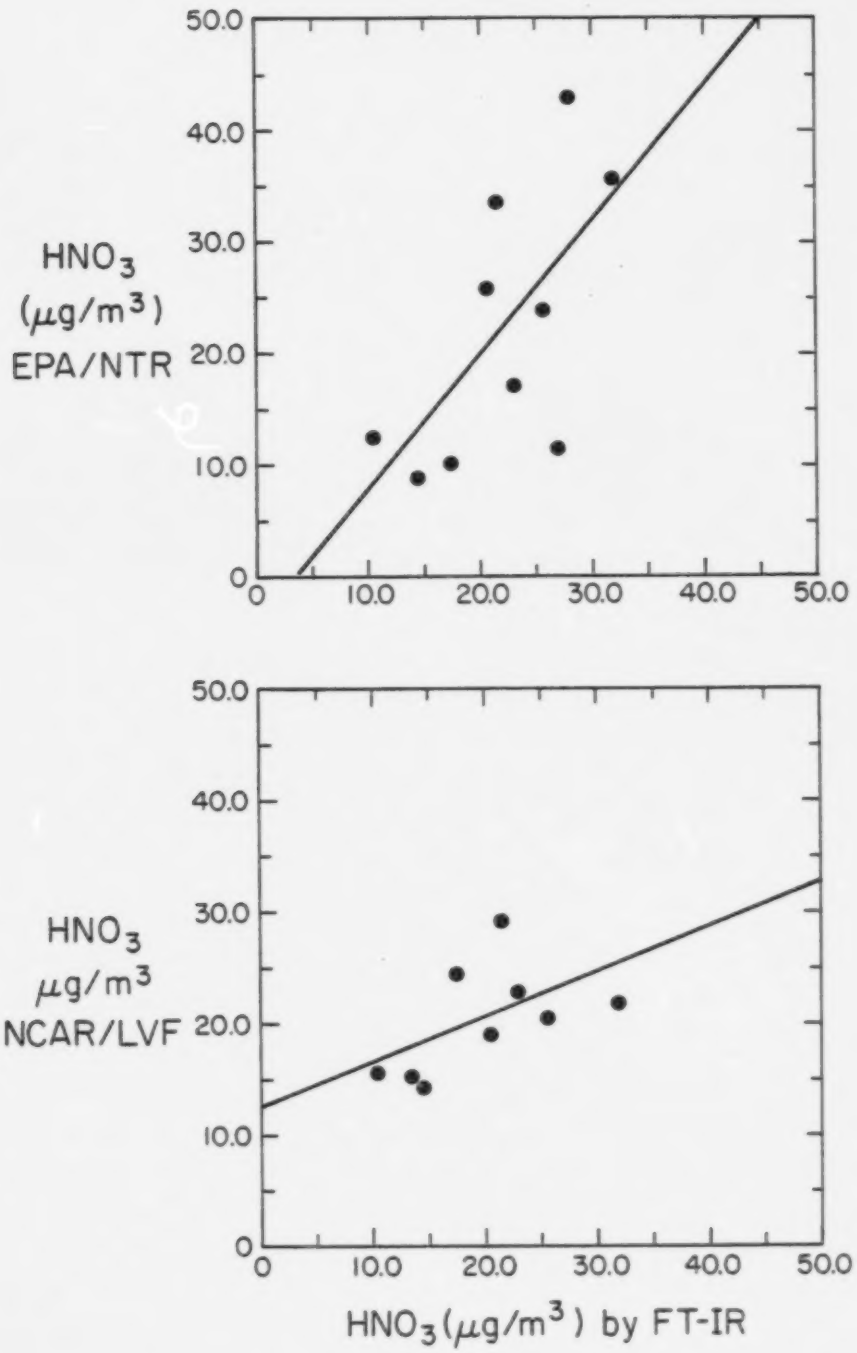

Figure 17. Regression fits of the FT-IR HNO_3 data with those obtained by the EPA/NTR and NCAR/LVF methods.

TABLE 9. REGRESSION FITS FOR NITRIC ACID WITH THE FT-IR DATA AS STANDARD

Method*	Intercept	Slope	Mean Square Error	Correlation Coeff. (R)
BAT/CHEM	2.14(±2.95)	0.86(±.12)	10.80	.91
BAT/LVF	2.65(±4.92)	1.15(±.21)	29.84	.88
BNL/LVF	-4.44(±5.92)	1.23(±.25)	42.94	.85
BNL/HVF	-0.85(±4.13)	0.95(±.17)	21.16	.87
BNL/DDE	-2.53(±6.43)	1.06(±.27)	50.67	.79
EPA/NTR	-4.32(±11.42)	1.20(±.50)	96.09	.65
EPA/TFDDE2	-4.29(±14.62)	1.03(±.54)	89.30	.62
NCAR/LVF	12.34(±4.84)	0.40(±.23)	19.24	.54

*See Table 5 for brief description of methods.

values are partly due to lack of sufficient "standard" data points below the 6 ppb (~15 $\mu g\ m^{-3}$) FT-IR detection limit. Among the methods treated in Table 9, NCAR/LVF is the only one which shows relatively poor intercept and slope (standard errors do not encompass 0 and 1, respectively) despite good precision in the results. The best comparison figures appear to be those for BAT/CHEM, which were obtained from one of two continuous chemiluminescence analyzers employed (Table 5) during the study. With few exceptions, the instantaneous readings of the BAT/CHEM instrument fall within ±4 ppb (the FT-IR measurement error for HNO_3) of the individual FT-IR values throughout the study (82).

The full interpretation of the nitric acid intercomparison data along with its implications for the data simultaneously gathered for particulate nitrate will be detailed in a forthcoming EPA report (83). The brief analysis presented here demonstrates the utility of long-path FT-IR spectroscopy, within its well-defined detection sensitivity, as a reliable and proven analytical method for measurements of gaseous pollutant concentrations against which other less well-tested techniques may be compared.

2. Other Collaborative Studies

In addition to the major field studies described above, the FT-IR facility, while in Claremont, was also involved in comparison tests with analytical methods for HNO_3, NH_3 and HCHO then being developed by workers from other research organizations. Thus, during the week of July 23-27, 1979, experiments were carried out with Dr. B. R. Appel (California Department of Health Services, Berkeley, CA) to evaluate his filter denuder-difference method for HNO_3 determination and his NH_3 measurements made by collection on oxalic acid coated filters (84). During the same period, workers from Rockwell International (Newbury Park, CA) also conducted tests of their method for ambient NH_3 analysis, which was likewise based on collecting samples on oxalic acid-impregnated filters. During several days in September 1979, Dr. G. Kok of Harvey Mudd College made a comparison of HCHO data obtained by his chemiluminescence apparatus against HCHO measurements by the FT-IR system.

E. Attempts to Detect Other Species

Nitrous Acid. It has been suggested (3,51) that HONO could form in NO_x-rich auto exhausts and be emitted in substantial quantities during the evening and early morning peak traffic hours. The ensuing sunlight photolysis of HONO, yielding OH radicals, would then enhance the initial rate of smog-forming reactions.

Two infrared bands of HONO, both with well-defined Q-branches of nearly equal intensities, lie within the accessible spectral window: the ν_4 fundamentals of trans-HONO and cis-HONO at 791 and 853 cm^{-1}, respectively. The absorptivity of the 853 cm^{-1} feature at 0.5 cm^{-1} resolution has been reported (51) as 71 cm^{-1} atm^{-1}. An absorptivity of ~30 cm^{-1} atm^{-1} for the 791 cm^{-1} trans-HONO band (Table 1) was derived using the reported (51) equilibrium ratio of [trans-HONO]/[cis-HONO] ~2.29 at 296 K. From these absorptivities we derive a detection limit of 10 ppb for cis + trans HONO at 1 km pathlength. However, HONO was not detected in the FT-IR spectra for the numerous episode days recorded throughout this study, including those where monitoring continued into the evening hours.

Recently, a highly sensitive long-path UV differential optical absorption spectrometer has been developed by researchers from Germany (85) for

the detection of specific trace species in the atmosphere at sub-ppb concentrations. Its use by Dr. U. Platt in Riverside during the summer of 1979 in collaboration with UC-SAPRC researchers resulted in the first detection of HONO in the polluted atmosphere. Levels of HONO of up to 4 ppb were reported for that period of study (86). Very recently, during a field study in downtown Los Angeles in July 1980, even higher concentrations of HONO were recorded during morning hours just before sunrise, with the highest concentration being ~7 ppb (87). These findings are consistent with our failure to detect HONO with the km-path FT-IR instrument given the 10 ppb detection limit which we established for this instrument.

Hydrogen Peroxide. The characterization of H_2O_2 levels in photochemical smog is of current interest in view of its suggested role as a chain terminator and as an index of hydroperoxyl (HO_2) radical concentrations (3,6,88). Early measurements of this species in ambient air employed the wet chemical $TiSO_4$ colorimetric method. Data gathered in 1970 (15,89,90) indicated H_2O_2 concentrations of up to 40 ppb in Hoboken, New Jersey and up to 180 ppb in Riverside, the latter measurement coinciding with a very severe smog episode in which the oxidant concentration reached 650 ppb. The LPIR measurements of Hanst et al. (9) in Pasadena indicated the possible presence of H_2O_2 at about 70 ppb during an intense episode in July 1973.

A joint study (12) of the H_2O_2 concentrations in Riverside air was conducted by workers from Harvey Mudd College, UC-SAPRC and EPA in July 1977. These new measurements employed the luminol-based chemiluminescent apparatus recently developed by Kok et al. (91) as well as two wet chemical methods: the $TiSO_4$ colorimetric method of Purcell and Cohen (92) used in the earlier studies by Gay and Bufalini (15) and the $TiCl_4$ colorimetric method of Pilz and Johann (93) adapted by UC-SAPRC workers for use in smog chamber experiments. Typical mid-afternoon concentrations of H_2O_2 during moderate smog episodes (O_3 ~150-200 ppb) were found to be in the range 10-20 ppb and the maximum H_2O_2 concentrations were observed at about the time of the O_3 maximum.

The above collaborative study was conducted at the location of our FT-IR facility and coincided with a number of our monitoring periods. A search for definitive H_2O_2 absorption features in our spectra yielded

negative results even from data corresponding to O_3 levels as high as 300 ppb. The results of the joint study indicated H_2O_2 levels of 20-30 ppb during the measurement period which overlapped with our FT-IR monitoring.

The infrared band of H_2O_2 which is most suitable for quantitative measurement is centered at 1267 cm^{-1}. The recently measured value of the absorptivity at 1250 cm^{-1} is 8.4 cm^{-1} atm^{-1} at 1 cm^{-1} resolution (59). At moderate relative humidities and pathlengths approaching 1 km, several neighboring H_2O lines are almost totally absorbing and produce severe distortion of the contour of this analytical band. In addition, mismatches between the methane contents of the reference clean air sample and that of the ambient air sample introduces the interfering P-branch of the 1310 cm^{-1} CH_4 fundamental. The maximum of this CH_4 P-branch also falls at 1250 cm^{-1} and is often stronger in the resulting ratio spectrum than the signal from the expected H_2O_2 levels.

At 0.5 cm^{-1} resolution, the well-resolved vibration-rotation lines of the H_2O_2 spectrum can provide positive identification of this compound. Unfortunately, the majority of these lines also overlap with the similarly resolved vibration-rotation lines of the CH_4 P-branch. Results of our attempts at eliminating these interferences through successive ratioing indicate that a minimum 3% absorption of the 1250 cm^{-1} feature at 0.5 cm^{-1} resolution must be present to establish positive detection of H_2O_2. This translates to a detection limit of 40 ppb and probably explains our non-detection of H_2O_2 since no concentrations above ~40 ppb were detected in the joint study cited above (12). The use of higher resolutions (e.g., 0.125 cm^{-1}) should improve the separation of the H_2O_2 fine structures from interfering H_2O and CH_4 lines and increase the absorptivity value such that a significant improvement in detection limit (probably to 10 ppb) may be possible.

Peroxynitric Acid. Among the various products observed from laboratory or smog chamber studies of air pollution related systems, peroxynitric acid ($HOONO_2$) is one of the most novel species identified to date. Although postulated by Simonaitis and Heicklen (94), it was first positively identified by Niki and co-workers (23) in an FT-IR study of Cl-atom sensitized oxidation of H_2-NO_2 mixtures, and later by Hanst and Gay (25) in a Cl_2-NO_2-HCHO system. Peroxynitric acid has also been observed in propene-NO_x

photooxidations (95). Although $HOONO_2$ has yet to be detected in ambient air, its discovery has led to great interest in its possible role in atmospheric chemistry (7,26-29).

The Q-branch absorption of $HOONO_2$ at 803 cm^{-1}, with a reported absorptivity (27) of 27 atm^{-1} cm^{-1} at 1 cm^{-1} resolution (approximately the same value as for 0.5 cm^{-1} resolution), is the only strong band of this compound which is accessible for km-pathlength FT-IR measurement. This peak resides on the shoulder of an intense water line and would require a 2% absorption for detection in our spectra corresponding to a detection limit of 8 ppb. Since laboratory and modeling studies (7,8) predict ambient, concentrations of $HOONO_2$ of less than 1 ppb, it is not expected that this compound would be observed by km pathlength FT-IR spectroscopy.

Detection Limits for Other Compounds.

a. RO_2NO_2. Since the discovery of peroxynitric acid (23), interest has grown in the search for its alkyl homologs in laboratory systems. Recent FT-IR studies have reported the observation of peroxyalkyl nitrates (31-32), such as CH_3OONO_2, $C_2H_5OONO_2$, $C_3H_7OONO_2$ and $(CH_3)_3CH_2\underset{O}{C}OONO_2$, in Cl-atom initiated reactions of alkane-NO_x mixtures. The compound $ClCOONO_2$ has also been observed in Cl-sensitized oxidation of CO-NO_x-air mixtures (30). The absorptions of these compounds in the readily accessible 800 cm^{-1} region are very similar to PAN in both position and intensity. However, the ambient concentration of PAN is expected to be much greater than the concentrations of RO_2NO_2 species (7,8) and our estimated detection limits at the 793 cm^{-1} band is ~6 ppb for the peroxyalkyl nitrates (twice that established for PAN).

b. N_2O_5. Based on smog chamber data (96), the heterogeneous reaction of N_2O_5 with H_2O has been suggested as the primary source of nitric acid in photochemical smog, with the HO + NO_2 reaction making only a minor contribution. Formation of N_2O_5 is initiated by the reaction of ozone with nitrogen dioxide to form NO_3:

$$NO_2 + O_3 \rightarrow NO_3 + O_2$$

followed by the equilibrium reaction

$$NO_2 + NO_3 \rightleftarrows N_2O_5 \quad \text{(fast)}$$

Measurements of N_2O_5 concentrations in the atmosphere would also provide information on the ambient concentrations of NO_3, since the equilibrium between these compounds is rapidly established at 300 K. However, the large photodissociation cross sections for NO_3 (97) in the solar actinic region indicate that N_2O_5 will have a relatively short lifetime at the ambient temperatures associated with smog episodes. Hanst and co-workers did not observe N_2O_5 during their Pasadena study (9) despite their reported detection sensitivity of 10 ppb. The sensitivity of the FT-IR method for N_2O_5 detection is not improved by employing kilometer pathlengths because the broad and relatively strong N_2O_5 bands at 740 and 1248 cm^{-1} are masked by totally absorbing CO_2 and H_2O bands. Thus, N_2O_5 is a case where modest spectral resolution (~2 cm^{-1}) and a shorter pathlength (~500 meters) will optimize detection conditions.

c. HCl. Trace quantities of hydrogen chloride have been reported in automobile exhaust as a combustion product of ethylene dichloride under certain operating conditions (98). Reactions of sea salt aerosol have also been suggested as a possible source of gas phase HCl (99). In addition, recent photooxidation studies (52,100) of chlorinated ethylenes showed HCl to be a major product. The fundamental absorption band of HCl is centered at 2886 cm^{-1} and is characterized by well-separated vibration-rotation lines, several of which are free of interferences by known atmospheric absorptions. From published line strengths (101), we estimate that the detection limit of our spectrometer for HCl is about 8 ppb. This sensitivity is probably not high enough to permit detection of HCl from the sources mentioned above and none was observed during the studies in Riverside and Claremont. Establishing upper limits for the ambient concentration of HCl in the present atmosphere is important in view of the imminent program of space shuttle launches in Southern California (vide supra).

d. CH_3CHO. Acetaldehyde has relatively weak absorption bands in the infrared spectral regions available to km-pathlength spectroscopy. Based on an approximate absorptivity for the 1113 cm^{-1} band derived from published spectra (102,103), our estimated minimum detectable concentration is about 60 ppb, well above expected ambient levels.

e. CH_2CHCHO. Measurements of acrolein in Los Angeles air by Altshuller and McPherson (14) in 1961 using colorimetric methods recorded an

average of 7 ppb and a maximum value of 14 ppb. Similar results were reported by Renzetti and Bryan (71). Using the absorption band at 959 cm^{-1}, our detection sensitivity for acrolein is ~15 ppb, but this compound was not observed in our studies.

f. $CH_2=C=O$. Ketene is formed from the reaction of ozone with propene and other alkenes (38,45). Estimates of an absorptivity for the 2151 cm^{-1} absorption band of ketene from published spectra (104,105) indicate a detection sensitivity of ~6 ppb for our system.

SECTION 5

CONCLUSIONS

This program has demonstrated the utility of long pathlength FT-IR spectroscopy for quantitatively measuring in ambient air parts-per-billion levels of nitrogenous and oxygenated compounds for which reliable alternate methods are either lacking or are just now being developed. Systematic application of this technique in studies of air pollution episodes in the California South Coast Air Basin succeeded in providing an extensive body of data on the ambient concentrations of some "noncriteria" pollutants, e.g., HNO_3, HCHO, HCOOH, PAN, NH_3, in photochemical smog. Detailed time-concentration profiles, obtained for each species in pollution episodes of differing intensity and duration as well as at two different monitoring sites (Riverside and Claremont), provide reliable reference data of comparative and predictive value which have been heretofore unavailable. Moreover, we believe that our simultaneous measurements (Tables A-10 to A-14) of HNO_3, HCHO, HCOOH, PAN, NH_3, and O_3 in Claremont, California during the 1978 smog season constitute the most comprehensive set of trace pollutant data currently available for use as a stringent test of chemical kinetic submodels in widely accepted urban airshed models.

Our results verified that HNO_3, and not PAN is the major nitrogen-containing product of photochemical smog and showed that HNO_3 levels correlate negatively with prevailing NH_3 concentrations. The data obtained in Riverside include numerous measurements of simultaneous NH_3 and HNO_3 concentrations; and these results support the hypothesis that particulate NH_4NO_3 is in equilibrium with its gas-phase precursors NH_3 and HNO_3. In areas such as Claremont where average NH_3 levels are significantly less (< 10 ppb), the HNO_3 concentration during the peak of a smog episode may be expected to amount to approximately 10% of the O_3 concentration or more.

Our data established that ambient concentrations of HCOOH are low and will rarely be above 20 ppb even during severe smog episodes. This is approximately 4-10 times lower than earlier values report from wet chemical and long-path FT-IR measurements. On the other hand, our results concur with early measurements by wet chemical techniques that high concentrations ($\geq$ 100 ppb) of HCHO may prevail during an intense siege of photochemical air pollution associated with high vehicular activity.

The collaborative studies conducted with workers from other research organizations in which our km pathlength FT-IR measurements of HNO_3, NH_3, and HCHO were used as benchmarks further attest to the value of long pathlength FT-IR spectroscopy as an analytical tool for air pollution studies. We note that this utility should not be limited to the characterization of species found in photochemical smog. Given the increasing awareness of the potential hazards posed by atmospheric releases of toxic materials and their degradation products, the long pathlength FT-IR technique should continue to serve as a highly developed method for atmospheric monitoring.

SECTION 6

RECOMMENDED IMPROVEMENTS IN INSTRUMENTATION

The extensive experience which we gained in the operation of the km-pathlength FT-IR facility during this four-year study enabled us to identify ways in which the present system could be improved to yield the best attainable performance in terms of sensitivity, as well as speed and convenience of data collection and processing. Most of the suggestions offered here apply not only to the particular case of atmospheric monitoring but also to long pathlength FT-IR studies conducted in laboratory and chamber systems.

A. Instrumentation

The use of second-generation IR interferometers and higher-capacity data systems is highly desirable. The Digilab Model 296 interferometer and data system used throughout this study is, by present standards, a slow and inefficient instrument. The fixed scanning velocity of the Model 296 is approximately 0.1 cm/sec; by contrast, the newer interferometers have selectable velocities of the moving mirror of up to ~3 cm/sec. The higher mirror velocity not only provides a higher rate of data collection, which is most needed at longer optical path difference (i.e., higher resolution), but is also a requisite for efficient matching with the frequency response of the more commonly employed low-temperature detectors (e.g., HgCdTe and InSb).

Complementing the high resolution ($\leq$ 0.125 cm^{-1}) capabilities of the new interferometers are advances in the data systems and peripherals. These include higher-capacity core memory ($\geq$ 32 K), moving head dual-disk drives, direct memory access (DMA), and special fast Fourier-transform (FFT) hardware. The overall result of these major improvements is an increase in the speed of data handling by better than an order of magnitude. For example, with the Digilab FTS-14 used in this study, co-addition of 30

interferograms (scans) at 0.5 cm^{-1} resolution takes ~6 minutes with a single-precision transform requiring about three minutes. By comparison, with a modern version of this instrument, such as those which are currently employed at UC-SAPRC, 60 scans at 0.125 cm^{-1} can be averaged in ~2 minutes, while transform computation with double precision arithmetic is accomplished in ~5 minutes.

The maximum resolution capability (0.5 cm^{-1}) of the Digilab Model 296 interferometer was employed throughout the study. It was obvious, however, that a higher resolution ($\leq$ 0.25 cm^{-1}) would have provided better sensitivity (through the increased value of the absorptivity) and much improved separation of sharp absorption features for certain pollutant species (e.g., HCHO, NH_3, HNO_3, H_2O_2) from those of atmospheric H_2O, CO_2, and CH_4. In addition to the above advantages, the better defined shape of an absorption peak under high resolution results in an increase in the measurement precision.

At high resolutions and long optical paths, it is most important that there be a provision for assuring coherence in the co-added interferograms. Even with thermostatted interferometers, it cannot be assumed under field conditions that the relative phase of the white light and reference laser signals is maintained throughout a given set of scans. When this phase relationship varies considerably from scan to scan, the resulting transforms (spectra) are characterized by small wavenumber shifts. These are most noticeable in the ratioed spectra where they induce spurious difference peaks among narrow spectral features. Under these conditions, it is difficult to extract quantitative information from partially overlapped peaks since background absorptions cannot be properly matched. Fortunately, some instrument makers now incorporate methods which assure that data points within an accepted set of scans follow a specified degree of tolerance. One technique is to correlate the phase of each succeeding interferogram to that of the previous ones, a relatively slow process. The most efficient technique uses laser-to-white light phase counters built into the interferometer interface. Sampling is referenced to either the rising or falling edge of the laser square wave signal and the counters track whether the white light pulse has drifted past the edge chosen for sampling. A scan is immediately terminated when the latter occurs and the moving mirror is

returned without completing the scan, thus little time is lost before a new scan is initiated.

B. Detectors

The use of two separate detectors (HgCdTe and InSb) to cover the entire mid-infrared range is inconvenient and results in lost time, since two sets of scans must be recorded and the infrared beam must be alternately refocused on each detector element. Sandwich detector design, in which the InSb element is directly over the HgCdTe element in a single dewar, would eliminate the need for refocusing between data collection. However, two sets of scans are still required and the light input to the HgCdTe element must be transmitted through the InSb element which often results in a reduction of signal by as much as 50%. The ideal detector for atmospheric monitoring is Cu:Ge which covers the entire mid-infrared region at a detectivity slightly better than that of HgCdTe. The Cu:Ge detector must be operated at $\leq$ 20 K and therefore requires a relatively bulky housing and costly closed-cycle refrigeration unit which presents additional vibration problems. We have found that vibration can be sufficiently reduced and that the convenience and savings in labor and time are worth the extra investment. When cost is prohibitive, an alternative possibility is the use of a dual-element HgCdTe and InSb detector in a single dewar in which the elements are immediately adjacent to each other.

Another important consideration in the selection of a particular detector is its linearity. As mentioned above, our recent tests at UC-SAPRC indicated that ambient air monitoring can be carried out effectively at 0.125 cm^{-1} resolution with the use of modern instrumentation. At this high resolution, specific spectral features of pollutants such as HCHO, NH_3, and HNO_3 can be conveniently measured from the single-beam spectrum (without resort to ratioing), since these features become better defined and well isolated from background absorptions. In extracting quantitative information from the single-beam (transmission) spectra, it is important that the zero signal baseline be accurately defined. Nonlinear detectors are characterized by spectra in which totally absorbing bands extends significantly below the zero baseline. This nonlinear behavior contributes to photometric inaccuracy.

C. Graphics

Processing of the large number of spectra which are generated during extended monitoring periods cannot be efficiently done with the use of hard copy outputs of a plotter alone. The data system should include a graphics CRT terminal where essentially all data reduction can be carried out. It is important that the software designed for this purpose be capable of displaying all of the data points of the spectral region being examined. The graphic display features found in most commercial instruments are based on a smaller set of representative data points (thus leading to lower effective resolution) such that quantitative analysis on the CRT screen only produces correct results when broad absorption bands are involved.

D. Multiple Reflection Optical System

The eight-mirror multiple-reflection optics designed by Hanst (53) and used in this study can be replaced with a more economical design which will result in about 50% reduction in the cost of optical components. The latter design follows Horn and Pimentel's (106) modification of the White optics by addition of a corner reflector immediately adjacent to the in-focus (nesting) mirror. The corner reflector serves to displace vertically the output beam of the normal White optics and feeds it back to the two out-of-focus (collecting) mirrors, effectively doubling the pathlength attainable in the conventional White cell. The arrangement is thus equivalent to the eight-mirror design. The fewer mirrors involved necessarily result in a simpler alignment procedure and further cost savings in mirror mount hardware.

Gold is traditionally the coating of choice for long-pathlength infrared work because of its high reflectivity (~99%) when freshly applied. Its use under the severe conditions of ambient air monitoring causes it to eventually degrade and become unusable even after repeated washings with solvents. Several companies are now offering a metal/dielectric coating with a specified reflectivity of 99.4% from 3.3 m to the far-infrared. The coating consists of silver overcoated with thorium fluoride and can be repeatedly cleaned without loss of reflectivity. Thorium fluoride is known to be a durable material and resists even HF in the vapor phase. The cost of the new coating is now competitive with that of gold.

The mirror mounts and adjustments must provide stable optical alignment over a wide temperature range. The original mirror mount design for the

eight-mirror long pathlength optics relied on springs to support the weight of each mirror as well as to provide the tension working against the adjustment screws. This arrangement was quite sensitive to temperature and invariably required several realignments during the course of a day's experiments. In a recently constructed long pathlength cell at UC-SAPRC, we employed a mounting system in which the weight of the mirror is totally supported by its central pivot. The latter consists of a ball socket, attached to the center of the mirror backing plate, which rests and pivots on a ball end whose stem is secured to the support frame. The orthogonal adjustments are provided by micrometer screws which track on V-grooves and work against the positive action of a single compression spring. Our tests indicated that this mirror mount design would provide alignment stability within temperature fluctuations of $\pm$ 15°C. This type of mounting was also implemented for the heavy collecting (out-of-focus) mirrors of the Hanst's optics during our last year of study in Claremont.

In summary, what is described in the above discussion are the salient features of an optimized long pathlength FT-IR facility: a state-of-the-art interferometer with high-speed data system, a high-performance detector covering the entire mid-infrared region, multiple-reflection optics of the highest possible reflectivity and provided with an exceptionally stable mounting system, and special software for rapid spectral analysis.

REFERENCES

1. K. Westberg and N. Cohen, "The Chemical Kinetics of Photochemical Smog as Analyzed by Computer," Report No. ATR-70-(8107)-1, Aerospace Corp., El Segundo, CA, December, 1969.

2. H. Niki, E. E. Daby and B. Weinstock, Adv. Chem. Ser., 113, 16 (1972).

3. K. L. Demerjian, J. A. Kerr and J. G. Calvert, "The Mechanism of Photochemical Smog Formation," in Advances in Environmental Science and Technology, Vol. 4, J. N. Pitts, Jr. and R. Metcalf, eds., Wiley-Interscience, New York, pp. 1-262 (1974).

4. T. A. Hecht, J. H. Seinfeld and M. C. Dodge, Environ. Sci. Technol., 8, 327 (1974).

5. T. E. Graedel, L. A. Farrow and T. A. Weber, Atmos. Environ., 10, 1095 1976.

6. G. Z. Whitten, J. P. Kilms and H. Hogo, "Modeling of Simulated Photochemical Smog with Kinetic Mechanisms," Systems Applications Inc., EPA-600/3-80-028a, February 1980.

7. A. C. Baldwin, J. R. Barker, D. M. Golden and D. G. Hendry, J. Phys. Chem., 81, 2483 (1977).

8. W. P. L. Carter, A. C. Lloyd, J. L. Sprung and J. N. Pitts, Jr., Int. J. Chem. Kinetics, 11,45 (1979).

9. P. L. Hanst, W. E. Wilson, R. K. Patterson, B. W. Gay, Jr., L. W. Chaney and C. S. Burton, A Spectroscopic Study of California Smog, Environmental Protection Agency, EPA Publication No. 650/4-75-0006, Research Triangle Park, NC (1975).

10. D. F. Miller and C. W. Spicer, J. Air Pollut. Control Assoc., 25, 940 (1975).

11. C. W. Spicer, "The Fate of Nitrogen Oxides in the Atmosphere," in Advances in Environmental Science and Technology, Vol. 7, J. N. Pitts, Jr., and R. Metcalf, eds., Wiley-Interscience, New York, pp. 163-262 (1977).

12. G. L. Kok, K. R. Darnall, A. M. Winer, J. N. Pitts, Jr. and B. W. Gay, Jr., Environ. Sci. Technol., 12, 1077 (1978).

13. P. P. Mader, G. Cann and L. Palmer, Plant Physiol., 30, 318 (1955).

14. A. P. Altshuller and S. P. McPherson, J. Air Pollut. Control Assoc., 13, 109 (1963).

15. B. W. Gay, Jr. and J. J. Bufalini, Adv. Chem. Ser., 113, 255 (1972).

16. Air Quality Criteria for Ozone and Other Photochemical Oxidants, Vol. I, Draft No. 2, U. S. Environmental Protection Agency, Office of Research and Development, Washington, DC 20460, January, 1978.

17. A. Q. Eschenroeder and J. R. Martinez, Advan. Chem. Ser., 113, 191 (1972).

18. G. Z. Whitten and H. Hogo, Mathematical Modeling of Simulated Photochemical Smog, EPA-60013-77-011, January, 1977.

19. A. C. Lloyd, "Tropospheric Chemistry of Aldehydes" Presented at Workshop on Chemical Kinetic Data Needs for Modeling the Lower Troposphere, Reston, VA, May 15-17, 1978, National Bureau of Standards Special Publication 557, p. 27.

20. G. A. Dawson, J. Geophys. Res., 82, 3125 (1977).

21. A. M. Winer, J. W. Peters, J. P. Smith and J. N. Pitts, Jr., Environ. Sci. Technol., 8, 1118 (1974).

22. D. F. Miller and C. W. Spicer, Paper No. 74-247, 67th Annual Meeting of the Air Pollution Control Association, Denver, CO, June 9-13, 1974.

23. H. Niki, P. D. Maker, C. M. Savage and L. P. Breitenbach, Chem. Phys. Lett., 45, 564 (1977).

24. R. Simonaitis and J. Heicklen, Int. J. Chem. Kinetics, 10 67 (1978).

25. P. L. Hanst and B. W. Gay, Environ. Sci. Technol., 11, 1105 (1977).

26. S. Z. Levine, W. M. Uselman, W. H. Chan, J. G. Calvert and J. H. Shaw, Chem. Phys. Lett., 48, 528 (1977).

27. R. A. Graham, A. M. Winer and J. N. Pitts, Jr., Chem. Phys. Lett., 51, 215 (1977).

28. R. A. Cox, R. G. Derwent and A. J. L. Hutton, Nature, 270, 328 (1977).

29. R. A. Graham, A. M. Winer and J. N. Pitts, Jr., J. Chem. Phys., 68, 4505 (1978).

30. J. W. Spence, E. O. Edney and P. L. Hanst, Chem. Phys. Lett., 56, 478 (1978).

31. H. Niki, P. D. Maker, C. M. Savage and L. P. Breitenbach, Fourier Transform IR Studies of Gaseous and Particulate Nitrogenous Compounds of Atmospheric Interest, presented at the 175th National Meeting of the ACS Division of Environmental Chemistry, Anaheim, CA, March 12-17, 1978.

32. E. O. Edney, J. W. Spence and P. L. Hanst, Peroxynitrates that can be formed in Polluted Air, presented at the 175th ACS National Meeting of ACS Division of Environmental Chemistry, Anaheim, CA, March 12-17, 1978.

33. O. C. Taylor, private communication (1978).

34. D. Grosjean, Chemical Transformations, Chap. IV-C, Review prepared for the Subcommittee on Ammonia, National Academy of Sciences, Committee on Medical and Biological Effects of Environmental Pollutants, Washington, DC (1977).

35. G. M. Hidy (ed.), "Characterization of Aerosols in California," ACHEX Final Report, Vol. I, September 30, 1974.

36. E. R. Stephens, P. L. Hanst, R. C. Doerr and W. E. Scott, Ind. Eng. Chem., 48, 1498 (1956).

37. E. R. Stephens, W. E. Scott, P. L. Hanst and R. C. Doerr, (a) Proc. Amer. Petrol. Inst., 30, 288 (1956). (b) J. Air Pollut. Control Assoc., 6, 159 (1956).

38. W. E. Scott, E. R. Stephens, P. L. Hanst and R. C. Doerr, Proc. Amer. Petrol. Inst., 37 (III), 171 (1957).

39. E. R. Stephens, P. L. Hanst, R. C. Doerr and W. E. Scott, J. Air Pollut. Control Assoc., 8, 333 (1959).

40. J. U. White, J. Opt. Soc. Amer., 32, 285 (1942).

41. E. R. Stephens and E. A. Schuck, Chem. Eng. Prog., 54, 71 (1958).

42. E. F. Darley, E. R. Stephens, J. T. Middleton and P. L. Hanst, Int. J. Air Pollut., 1, 155 (1959).

43. E. R. Stephens and W. E. Scott, Proc. Amer. Petrol. Inst., 42, (III) 665 (1962).

44. J. M. Heuss and W. A. Glasson, Environ. Sci. Technol., 2, 1109 (1968).

45. P. L. Hanst, E. R. Stephens, W. C. Scott and R. C. Doerr, Atmospheric Ozone Reactions, The Franklin Institute (1958), Philadelphia, PA.

46. S. L. Kopczynski and J. J. Bufalini, Anal. Chem., 43, 1126 (1971).

47. J. N. Pitts, Jr., J. M. McAfee, W. D. Long and A. M. Winer, Environ. Sci. Technol., 10, 787 (1976).

48. J. M. McAfee, E. R. Stephens, D. Fitz and J. N. Pitts, Jr., J. Quant. Spectrosc. Radiat. Transfer, 16, 829 (1976).

49. H. Niki, P. Maker, C. Savage and L. Breitenbach, Fourier Transform Spectroscopic studies of Organic Species Participating in Photochemical Smog Formation, in Conference on Environmental Sensing and Assessment, Las Vegas, NV, September 14-19, 1975.

50. H. Niki, P. Maker, C. M. Savage and L. P. Breitenbach, Chem. Phys. Lett.,46, 327 (1977).

51. H. W. Chan, R. J. Nordstrom, J. G. Calvert and J. H. Shaw, Environ. Sci. Technol., 10, 674 (1976).

52. B. W. Gay, Jr., P. L. Hanst, J. J. Bufalini and R. C. Noonan, Environ. Sci. Technol., 10, 58 (1976).

53. P. L. Hanst, "Spectroscopic Methods for Air Pollution Measurements," in Advances in Environmental Science and Technology, Vol. 2, J. N. Pitts, Jr. and R. L. Metcalf, eds., Wiley-Interscience, New York, pp. 257-300 (1980).

54. P. L. Hanst, A. S. Lefohn and B. W. Gay, Jr., Appl. Spectrosc., 27, 188 (1973).

55. G. J. Doyle, P. J. Bekowies, A. M. Winer and J. N. Pitts, Jr., Environ. Sci. Technol., 11, 45 (1977).

56. A. M. Winer, R. A. Graham, G. J. Doyle, P. J. Bekowies, J. M. McAfee and J. N. Pitts, Jr., "An Evacuable Thermostatted Environmental Chamber and Solar Simulator Facility for the Study of Atmospheric Chemistry," in Advances in Environmental Science and Technology, Vol. 10, J. N. Pitts, Jr. and R. L. Metcalf, eds., Wiley-Interscience, New York, pp. 461-511 (1980).

56. R. A. Graham, Software for UC-SAPRC's FT-IR System (1977, unpublished).

57. E. R. Stephens, Anal. Chem., 36, 928 (1974).

58. H. W. Chan, R. J. Nordstrom, J. G. Calvert and J. H. Shaw, Environ. Sci. Technol., 10, 674 (1976).

59. L. Molina and M. Molina, unpublished results (1980).

60. E. C. Tuazon, R. A. Graham, A. M. Winer, R. R. Easton, J. N. Pitts, Jr. and P. L. Hanst, Atmos. Environ., 12, 865 (1978).

61. E. C. Tuazon, A. M. Winer, R. A. Graham and J. N. Pitts, Jr., "Atmospheric Measurements of Trace Pollutants by Kilometer-Pathlength FT-IR

Spectroscopy," in Advances in Environmental Science and Technology, Vol. 10, J. N. Pitts, Jr. and R. L. Metcalf, eds., Wiley-Interscience, New York, pp. 259-300 (1980).

62. D. Grosjean, G. J. Doyle, T. M. Mischke, M. M. Poe, D. R. Fitz, J. P. Smith and J. N. Pitts, Jr., The Concentration, Size Distribution and Modes of Formation of Particulate Nitrate, Sulfate and Ammonium Compounds in the Eastern Part of the Los Angeles Basin, 69th Annual Meeting of the Air Pollution Control Association, Portland, OR, June 27-July 1, 1976.

63. D. Grosjean, J. P. Smith, T. M. Mischke and J. N. Pitts, Jr., in Atmos. Pollut., M. M. Benarie, ed., Elsevier, Amsterdam, pp. 549-563 (1976).

64. "JANAF Thermochemical Tables," 2nd ed., NSRDS-NBS 37, 1971.

65. D. D. Wagman, W. H. Evans, V. B. Parker, I. Harlow, S. M. Bailey and R. H. Schumm, "Selected Values of Chemical Thermodynamic Properties," NBSTN 270-3, 1968

66. S. W. Benson, "Thermochemical Kinetics", Second edition, Wiley, New York, (1976).

67. G. J. Doyle, E. C. Tuazon, R. A. Graham, T. M. Mischke, A. M. Winer and J. N. Pitts, Jr., Environ. Sci. Technol., 13, 1416 (1979).

68. P. L. Hanst, J. W. Spence, M. Miller, Environ. Sci. Technol., 11, 403 (1977).

69. E. C. Tuazon, A. M. Winer, R. A. Graham, J. P. Schmid and J. N. Pitts, Jr., Environ. Sci. Technol., 12, 954 (1978).

70. A. P. Altshuller, J. Air Pollut. Control Assoc., 28, 594 (1978).

71. N. A. Renzetti and R. J. Bryan, J. Air Pollut. Control Assoc., 11, 421 (1961).

72. G. R. Lyles, F. B. Dowling and V. J. Blanchard, J. Air Pollut. Control Assoc., 15, 106 (1965).

73. W. S. Cleveland, T. E. Graedel and B. Kleiner, Atmos. Environ., 11, 357 (1977).

74. C. Morley and I. W. Smith, J. Chem. Soc. Faraday Trans. II, 68, 1016 (1972).

75. A. E. Orel and J. H. Seinfeld, Environ. Sci. Technol., 11, 1000 (1977).

76. G. M. Hidy, J. Air Pollut. Control Assoc., 25, 1106 (1975).

77. D. Grosjean and S. K. Friedlander, J. Air Pollut. Control Assoc., 25, 1038 (1975).

78. B. R. Appel, E. L. Kothny, E. M. Hoffer, G. M. Hidy and J. J. Wesolowski, Environ. Sci. Technol., 12, 418 (1978).

79. L. W. Richards, private communication (1979).

80. R. K. Stevens (Ed.), "Handbook on Measurement of Atmospheric Nitrates," EPA-RTP, N.C. (1978).

81. Battelle, Columbus Laboratories, "Preliminary Report of the Results of the Claremont Inter-Comparison Study of Nitric Acid and Particulate Nitrate Measurement Methods," prepared for the symposium held at EPA-RTP on May 20, 1980.

82. C. W. Spicer, private communication (1980).

83. R. K. Stevens, private communication (1980).

84. B. R. Appel, Y. Tokiwa and M. Haik, Atmos. Environ., submitted for publication, (1980).

85. U. Platt, D. Perner and H. W. Pate, J. Geophys. Res., 84, 6329 (1979).

86. U. Platt, D. Perner, G. W. Harris, A. M. Winer and J. N. Pitts, Jr., Nature, 285, 312 (1980).

87. D. Perner, U. Platt, G. W. Harris, N. Miller, W. D. Long, A. M. Winer and J. N. Pitts, Jr., unpublished results, 1980.

88. J. J. Bufalini and K. Brubaker, Symposium on Chemical Reactions in Urban Atmospheres, Research Laboratories, General Motors Corp., Warren, MI, October 6-7, 1969.

89. J. J. Bufalini, B. W. Gay, Jr. and S. L. Kopczynski, Environ. Sci. Technol., 5, 33 (1971).

90. J. J. Bufalini, B. W. Gay, Jr. and K. L. Brubaker, Environ. Sci. Technol., 6, 816 (1972).

91. G. L. Kok, T. Haller, M. Lopez, H. Nachtreib and M. Yuan, Environ. Sci. Technol., in press (1978).

92. T. C. Purcell and I. R. Cohen, Environ. Sci. Technol., 1, 845 (1967).

93. W. Pilz and T. Johann, Int. J. Environ. Sci. Technol., 3, 257 (1974).

94. R. Simonaitis and J. Heicklen, J. Phys. Chem., 80, 1 (1976).

95. J. N. Pitts, Jr., B. J. Finlayson-Pitts and A. M. Winer, Environ. Sci. Technol., 11, 568 (1977.

96. C. W. Spicer and D. F. Miller, J. Air Pollut. Control Assoc., 26, 45 (1976).

97. R. A. Graham and H. S. Johnston, J. Phys. Chem., 82, 254 (1978).

98. R. Campion, private communication (1976).

99. S. K. Friedlander, Environ. Sci. Technol., 7, 235 (1973).

100. J. P. Heicklen, E. Sanhueza, I. C. Hisatsune, P. K. Jayanty, R. Simonaitis, L. A. Hull, C. W. Blume and E. Mathias, "Oxidation of Halocarbons," Final Report, EPA Grant #R800949, May 1975.

101. R. A. Toth, R. H. Hunt and E. K. Plyler, J. Mol. Spectrosc., 35, 110 (1970).

102. J. C. Evans and H. J. Bernstein, Can. J. Chem., 34, 1083 (1956).

103. D. S. Erley and B. H. Blake, "Infrared Spectra of Gases and Vapors," Vol. II, The Dow Chem. Co., Midland, MI (1965).

104. W. F. Prendale and W. H. Fletcher, J. Chem. Phys., 26, 793 (1957).

105. W. R. Harp, J. and R. S. Rasmussen, J. Chem. Phys., 15, 778 (1974).

106. D. Horn and G. C. Pimentel, Appl. Optics, 10, 7892 (1971).

APPENDIX A

Ambient Air Measurements

TABLE A-1. POLLUTANT CONCENTRATIONS* (PPB) IN RIVERSIDE AIR, 1976 STUDY

DATE	TIME (PDT)	O_3	NH_3	PAN	HCOOH	HCHO†	HNO_3
Oct. 4	1033	52	8	5	-		-
	1208	85	7	4	-	-	-
	1252	89	4	4	-	-	-
	1511	113	43	5	-	-	-
	1603	145	33	7	2	-	-
	1700	228	25	18	3	6	-
	1730	220	6	14	3	13	-
	1759	213	-	14	5	11	-
	1827	203	-	13	4	-	-
	1903	106	-	8	2		-
	1913	78	-	5	2		-
Oct. 5	1552	140	50	4	-	6	-
	1634	285	29	15	2	14	-
	1705	258	21	15	3	11	-
	1736	218	28	12	3	14	-
	1805	210	19	12	3	10	-
	1833	205	-	13	7	13	6
	1922	150	-	10	5	10	8
	1947	123	-	9	3		6
Oct. 6	1142	150	6	11	5		8
	1155	170	6	11	5	-	6
	1258	120	19	11	-		7
	1320	115	32	3	-	-	6
	1429	185	60	6	-		6
	1514	218	43	3	3	6	-
	1556	190	31	12	2	-	-
	1630	187	29	9	2	6	-
	1658	200	42	9	3	11	-
	1725	192	35	9	2	8	-
	1753	185	36	9	2	11	-
	1833	125	17	7	2		-
	1853	108	4	7	2		-

*Dashes indicate below detection limit: O_3, 10 ppb; NH_3, 4 ppb; PAN, 3 ppb; HCOOH, 2 ppb; HCHO, 6 ppb; HNO_3, 6 ppb.

†Formaldehyde measurements were made with the InSb detector approximately 10-15 min after the times in the table for the HgCdTe detector spectra.

TABLE A-2. POLLUTANT CONCENTRATIONS* (PPB) IN RIVERSIDE AIR
July 21, 1977

Time†	O_3	PAN	NH_3	HNO_3	HCOOH	HCHO‡	NO_2	NO	NMHC# (ppmC)	CO (ppm)
1140	173	10	--	--	3	15	40	1	0.3	1.2
1202	180	8	—	--	3	12	36	1	0.3	1.4
1231	165	4	—	--	4	11	35	1	0.2	1.1
1258	161	3	4	--	2	13	28	2	0.2	0.8
1336	152	—	25	--	2	13	23	2	0.2	0.7
1423	198	3	41	--	2	11	36	2	0.1	1.0
1444	216	2	38	--	--	13	43	2	0.1	.9
1507	214	6	29	--	2	15	35	2	0.3	1.1
1534	245	5	24	10	1	15	37	3	0.3	1.2
1552	229	8	19	7	3	19	53	3	0.4	1.4
1610	253	9	13	9	5	20	37	2	0.4	1.5
1632	264	10	11	10	4	19	54	2	0.5	1.4
1653	238	9	5	--	4	19	65	2	0.5	1.5
1711	239	9	6	10	3		49	2	0.6	1.6
1743	239	9	6	--	4	18	66	2	0.4	1.3
1800	225	11	--	--	3	18	59	2	0.4	1.3
1818	200	9	9	12	4	17	55	2	0.4	1.3
1835	206	9	8	--	2	19	64	2	0.4	1.3
1857	181	9	8	—	2		83	2	0.4	1.3

*Dashes indicate below detection limit. Blanks indicate no measurements.

†Pacific daylight time.

‡Formaldehyde measurements were made with the InSb detector approximately 10-15 minutes after the times listed in the table for the HgCdTe detector spectra.

#Non-methane hydrocarbons expressed as parts-per-million carbon.

TABLE A-3. POLLUTANT CONCENTRATIONS (PPB) IN RIVERSIDE AIR, JULY 25, 1977

Time	O_3	PAN	NH_3	HNO_3	HCOOH	HCHO	NO_2
1058	137	3	—	8	2	11	
1128	145	—	—	8	3	11	
1210	158	—	8	8	—	12	
1229	142	—	7	9	2	16	
1308	130	—	29	—	—	15	
1350	193	—	47	—	—	13	
1500	51	—	14	—	—	9	
1542	189	—	24	9	—		
1603	256	9	13	15	3	16	51
1623	291	10	18	20	3	19	31
1642	247	8	19	17	4	16	55
1704	197	5	13	15	3	13	85
1722	191	5	14	12	2	19	59
1755	184	3	13	14	2	13	42

TABLE A-4. POLLUTANT CONCENTRATIONS (PPB) IN RIVERSIDE AIR, AUGUST 10, 1977

Time	O_3	PAN	NH_3	HNO_3	HCOOH	HCHO	NO_2
1333	157	6	39	--	4	7	22
1407	137	—	36	—	3	9	38
1458	226	4	40	--	4	13	28
1530	234	10	25	—	6	13	34
1600	129	7	20	--	5		103
1619						18	
1636*	164	6	6	--	6		88
1646	164	8	7	--	6		99
1656						17	
1706						19	
1717	229	9	--	--	7		72
1726	202	9	--	--	7		68
1736						14	
1745						18	
1755	183	7	--	--	6		54
1805	172	8	--	--	8		63
1815						17	
1825						17	
1837	147	8	4	--	6		69
1849						18	

*Pairs of entries that are single-spaced indicate comparison of measurements by first sampling with the blower on continuously and then with the blower off at the start of the next measurement.

TABLE A-5. POLLUTANT CONCENTRATIONS (PPB) IN RIVERSIDE AIR, AUGUST 11-12, 1977

Time	O_3	PAN	NH_3	HNO_3	HCOOH	HCHO	NO_2
August 11							
1157	159	—	13	8	5	27	48
1245	181	4	39	—	4	16	36
1330	171	4	33	—	4	11	31
1430	174	4	30	—	—	17	26
1500	268	8	37	8	9	20	42
1535	287	13	21	13	8	26	68
1554	196	10	14	10	7	21	64
1616	223	10	15	10	10	23	92
1635	266	10	13	9	9	23	75
1653	229	8	10	11	8	20	47
1716	174	11	9	9	10	23	73
1737	209	7	6	—	7		55
August 12							
1200	171	6	—	14	11	20	25
1232	181	7	15	16	10	19	25
1302	177	7	33	11	8	16	25
1330	195	8	38	9	8	18	25
1400	229	7	46	9	9	17	46
1430	241	8	32	—	8	25	72
1500	247	11	29	9	6	25	52
1530	249	11	32	9	7	22	54
1559	211	10	22	9	9	25	52
1629	182	4	20	10	4	9	74
1703	178	5	13	11	5		80
1712	182	6	9	10	7		61
1721						18	
1731						20	
1740	156	4	6	8	5		73
1749	156	7	7	9	6		81
1801						21	
1810						20	

TABLE A-6. POLLUTANT CONCENTRATIONS (PPB) IN RIVERSIDE AIR, OCTOBER 3-4, 1977

Time	O_3	PAN	NH_3	HNO_3	HCOOH	HCHO	NO_2
October 3							
1110	139	9	--	9	7	29	57
1130	157	10	—	12	8	27	57
1200	148	5	--	13	8	24	47
1230	125	--	—	12	5	16	19
1300	93	—	—	9	4	12	36
1330	154	--	—	8	3	14	24
1400	148	--	25	10	3		23
1433	129	--	57	—	2	13	47
1505	135	--	54	9	--	18	29
1527	162	7	43	--	5	21	88
1547	241	8	30	--	6	24	55
1615	160	7	30	--	6	19	84
1645	180	7	27	--	7	20	54
1710	162	7	24	--	5	24	81
October 4							
1135	125	5	--	--	3	22	46
1200	178	10	—	14	8	24	33
1230	180	10	—	14	6	19	34
1300	195	8	--	15	7	21	37
1333	170	4	--	15	5	15	22
1402	141	4	—	7	3	18	35
1434	159	—	—	10	3	19	26
1509	95	—	27	—	—	9	31
1530	136	--	34	—	—	14	38
1600	184	5	37	8	2	25	51
1630	178	6	28	9	5	23	78
1705	131	5	29	--	4	21	132

TABLE A-7. POLLUTANT CONCENTRATIONS (PPB) IN RIVERSIDE AIR, OCTOBER 11, 1977

Time	O_3	PAN	NH_3	HNO_3	HCOOH	HCHO	NO_2	NO	NMHC (ppmC)	CO (ppm)
1305	—	--	--	--	--	26	95	6	0.7	2.6
1324	123	4	6	12	5	21	62	4	0.5	3.1
1344	133	5	5	9	6	22	60	3	0.5	2.1
1410	125	4	27	--	3	20	60	2	0.4	1.7
1433	123	4	59	8	4	19	63	4	0.4	2.0
1502	159	4	107	--	4	18	48	2	0.3	1.4
1523	181	6	132	--	4	8	51	2	0.3	2.3
1550	180	5	102	--	4	12	47	2	0.3	1.2
1620	127	4	52	--	3	18	91	3	0.9	1.9
1644	174	8	49	--	6	30	118	3	0.6	2.2
1710	205	11	32	--	9	38	119	3	0.8	2.8
1730	223	13	31	--	8	35	97	3	0.8	3.2
1750	192	15	27	--	8	28	96	2	0.7	2.6
1817	242	16	26	--	8	26	66	2	0.8	3.0
1847	206	18	17	--	9	30	61	2	0.9	3.0
1910	132	16	14	--	8	22	67	2	0.4	2.7

TABLE A-8. POLLUTANT CONCENTRATIONS (PPB) IN RIVERSIDE AIR, OCTOBER 14, 1977

Time	O_3	PAN	NH_3	HNO_3	HCOOH	HCHO	NO_2	NO	NMHC (ppmC)	CO (ppm)
1205	76	--	—	--	5	14	116	9	0.7	2.7
1231	82	--	—	--	2	17	69	5	0.4	1.4
1300	112	—	—	--	--	8	50	3	0.3	1.2
1330	131	—	23	9	--	10	32	1	0.2	1.2
1402	105	—	90	--	--	—	59	4	0.2	0.7
1430	115	--	102	7	--	—	35	3	0.2	0.7
1500	195	6	93	8	3	18	55	2	0.3	1.2
1524	259	12	55	8	6	21	71	2	0.6	2.6
1544	260	11	46	8	7	21	57	2	0.6	4.7
1605	251	11	32	--	6	20	78	2	0.8	2.7
1630	242	12	27	--	7	34	107	2	0.7	2.8
1650	231	14	18	--	7	36	119	3	0.7	2.9
1710	221	15	25	--	10	35	133	3	1.1	4.0
1736	253	17	22	--	10	35	121	2	1.0	4.1
1756	227	17	21	--	12	35	127	3	1.0	4.3
1829	171	14	9	--	13	32	109	3	1.0	3.8
1850	133	16	--	—	11	33	94	3	1.1	3.9
1910	121	14	--	—	11	30	100	3	1.0	4.1

TABLE A-9. POLLUTANT CONCENTRATIONS (PPB) IN RIVERSIDE AIR, OCTOBER 17, 1977

Time	O_3	PAN	NH_3	HNO_3	HCOOH	HCHO	NO_2	NO	NMHC (ppmC)	CO (ppm)
1302	114	--	15	9	3	12	64	5	0.5	1.8
1331	115	--	20	11	4	11	55	3	0.3	2.9
1400	144	--	27	9	4	15	38	2	0.4	1.6
1430	141	--	38	—	3	—	43	2	0.2	1.4
1500	167	--	81	—	4	12	42	3	0.3	1.1
1531	199	8	68	—	6	18	66	2	0.5	2.1
1601	199	7	31	—	5	15	48	2	0.6	2.2
1630	220	7	26	—	6	25	51	2	0.5	2.1
1650	231	10	16	—	8	25	65	2	0.6	2.4
1713	240	12	14	—	10	23	84	2	1.1	3.3
1738	187	14	15	—	10	35	115	2	0.9	3.7
1800	188	13	13	—	10	38	105	3	0.8	3.5
1830	140	13	4	--	11	25	101	3	0.9	4.6
1900	96	13	--	—	10	28	137	5	1.0	3.8

TABLE A-10. POLLUTANT CONCENTRATIONS* (PPB) IN CLAREMONT AIR ON OCTOBER 9, 1978

TIME†	O_3	PAN	HNO_3	NH_3	HCOOH	HCHO‡
1000	-	-	12	6	5	23
1030	16	-	12	6	4	18
1100	34	-	12	11	2	
1130	48	-	14	11	2	19
1200	38	-	12	5	2	15
1230	41	-	6	-	2	13
1300	66	-	15	9	2	20
1330	63	-	15	11	2	10
1400	47	-	10	8	-	6
1430	57	-	12	8	-	13
1500	88	-	17	6	2	12
1530	101	-	14	-	-	17
1600	163	6	17	7	2	17
1630	152	5	18	5	4	18
1700	117	3	16	7	2	14
1800	19	-	14	11	2	19
1900	-	3	11	10	5	20
2000	-	-	10	-	4	21
2100	-	-	7	-	4	23

*Dashes indicate below detection limit. Blanks indicate no measurements.

†Pacific daylight time.

‡Formaldehyde measurements were made with the InSb detector within 15 minutes after the times listed for the HgCdTe detector spectra.

TABLE A-11. POLLUTANT CONCENTRATIONS (PPB) IN CLAREMONT AIR ON OCTOBER 10, 1978

TIME	O_3	PAN	HNO_3	NH_3	HCOOH	HCHO
1000	30	-	13	9	4	20
1030	39	-	13	8	5	26
1100	58	-	15	8	4	21
1130	78	3	13	17	2	20
1200	58	-	12	23	-	17
1230	59	-	10	9	-	15
1300	53	-	10	10	-	12
1330	75	-	11	10	-	12
1400	94	3	17	7	2	14
1430	117	5	15	8	2	18
1500	227	14	28	9	2	30
1530	153	6	21	10	3	18
1600	102	3	18	11	4	13
1630	83	-	12	8	2	16
1700	43	-	12	6	-	7
1730	43	-	13	9	3	19
1800	32	-	12	-	2	21
1830	10	-	7	10	2	19
1900	-	-	10	8	4	23
1930	-	-	10	-	4	21
2000	-	-	6	9	3	21

TABLE A-12. POLLUTANT CONCENTRATIONS (PPB) IN CLAREMONT AIR ON OCTOBER 11, 1978

TIME	O_3	PAN	HNO_3	NH_3	HCOOH	HCHO
0900	-	-	10	8	4	27
0930	-	-	11	11	4	27
1000	23	-	12	6	4	27
1030	42	-	13	7	3	24
1100	56	-	14	11	3	23
1130	88	-	17	13	2	18
1200	99	3	22	11	2	21
1230	110	3	19	9	-	23
1300	104	3	18	8	-	18
1330	125	4	15	9	2	23
1400	122	4	18	9	3	19
1430	147	4	20	6	3	20
1500	183	6	23	4	3	
1530	235	8	26	7	3	31
1600	280	13	30	11	7	31
1630	210	10	26	8	6	25
1700	115	6	20	10	2	17
1735	88	4	11	4	3	22
1800	84	4	11	6	4	24
1830	64	5	9	-	5	28
1900	12	6	9	6	5	31
1930	10	5	9	7	4	29
2000	22	4	8	5	5	20

TABLE A-13. POLLUTANT CONCENTRATIONS (PPB) IN CLAREMONT AIR ON OCTOBER 12, 1978

TIME	O_3	PAN	HNO_3	NH_3	HCOOH	HCHO
1000	62	3	14	6	4	32
1030	65	4	14	9	2	31
1100	91	3	17	6	3	20
1130	105	3	16	9	3	19
1200	106	-	16	9	2	
1230	130	-	19	7	3	23
1300	152	3	20	8	2	25
1330	148	4	20	8	2	24
1400	151	4	17	11	2	19
1430	135	3	14	11	-	18
1500	209	6	19	13	2	25
1530	186	4	22	10	2	22
1605	225	7	27	9	3	28
1630	264	10	29	5	6	36
1700	281	11	29	10	8	51
1725	360	22	28	6	13	51
1748	299	21	27	8	15	52
1813	193	18	23	8	15	52
1834	145	17	22	7	15	47
1900	88	17	21	5	17	45
2000	38	18	21	5	14	46
2030	53	18	14	4	16	47
2105	10	15	13	-	14	40
2207	-	11	8	4	11	40
2251	-	10	7	7	9	41
2325	-	8	9	7	7	33

TABLE A-14. POLLUTANT CONCENTRATIONS (PPB) IN CLAREMONT AIR ON OCTOBER 13, 1978

TIME	O_3	PAN	HNO_3	NH_3	HCOOH	HCHO	NO_2*	NO*
0007	15	8	8	-	7	26	86	-
0039	-	8	8	7	7	21	80	4
0110	11	4	-	5	7	17	56	-
0137	21	4	6	8	7	22	38	-
0203	40	5	9	-	6	15	30	-
0233	14	4	6	-	5	18	43	-
0305	13	6	-	6	7	21	71	-
0332	-	6	-	7	8	19	64	-
0401	14	5	-	7	6	22	43	-
0453	-	3	-	6	4	18	64	5
0523	-	-	-	7	4	17	40	-
0549	-	-	-	5	3	22	60	6
0619	-	-	6	7	2	18	73	12
0652	-	-	-	6	2		79	30
0720	-	-	6	-	2	20	156	90
0746	-	-	10	7	5	20	230	144
0812	-	-	10	6	5	27	146	54
0840	15	3	11	7	7	39	142	36
0920	35	6	20	8	8	36	106	7
0942	19	5	17	-	7	37	165	17
1004	29	6	17	7	10	40	179	18
1030	60	5	18	10	7	40	157	8
1100	96	9	21	12	7	36	170	5
1130	131	8	26	14	6	41	146	4
1200	132	8	24	12	5	40	158	4
1230	168	12	31	20	5	43	151	2
1300	207	12	28	13	8	35	134	1
1330	237	13	29	14	8	37	109	1
1406	252	10	28	14	6	36	98	-
1432	270	11	28	25	6	42	101	-

(continued)

TABLE A-14. (continued) - 2

TIME	O_3	PAN	HNO_3	NH_3	HCOOH	HCHO	NO_2*	NO*
1503	296	16	27	20	8	55	127	-
1527	382	27	44	11	13	68	145	-
1550	412	31	48	10	17	70	175	1
1618	454	37	49	11	18	71	144	-
1642	392	32	44	9	19	66	160	-
1715	223	20	37	9	17	61	193	1
1745	206	22	39	7	15	53	173	-
1810	133	20	33	10	16	51	162	-
1833	78	15	23	9	13	43	171	-
1900	39	11	21	6	12	37	171	-
2009	-	16	14	-	13	34	222	40
2033	-	8	12	10	11	34	220	37
2103	-	6	10	6	9	35	218	35
2132	-	7	10	8	8	37	237	48
2208	-	7	8	8	8	34	147	20
2235	-	7	8	9	7	35	153	16
2303	-	6	6	9	7	35	161	25
2335	-	4	-	-	6	30	97	13

*NO_x measurements are instantaneous readings from a TECO chemiluminescence analyzer. Reported values for NO_2 are corrected for interferences due to PAN and HNO_3.

TABLE A-15. CONCENTRATIONS (PPB) OF NITRIC ACID, AMMONIA, AND FORMALDEHYDE IN CLAREMONT AIR DURING THE PERIOD AUGUST 27-SEPTEMBER 3, 1979 AS MEASURED BY LONG-PATH FT-IR SPECTROSCOPY

TIME (PDT)	HNO_3	NH_3	O_3* (ppb)	T(°C) AMBIENT	T(°C) CELL	% RH CELL	TIME (PDT)	HCHO
				AUGUST 27 (MONDAY)				
0600	-†	-	45	18.3	17.9	73.4	0615	10
0630	-	-	47	18.4	18.2	72.1		
0700	-	-	10	22.5	19.7	69.3	0715	8
0730	-	4	13	22.6	24.6	64.9		
0800	-	6	18	22.2	27.7	61.1	0820	22
0835	6	7	16	23.1	32.3	54.3		
0905	6	11	60	23.4	34.0	50.9	0920	17
0935	9	10	67	24.3	36.2	46.8		
1000	10	9	109	25.7	37.0	43.4	1018	16
1035	12	8	134	26.2	37.5	40.9	1115	18
1130	18	7	143	28.4	40.1	40.5		
1200	15	6	161	27.5	38.3	39.8	1218	16
1235	21	4	197	28.6	38.8	37.9		
1303	19	-	193	29.4	40.0	35.2	1318	10
1331	17	-	203	30.3	39.7	35.2		
1400	15	-	200	30.0	41.0	32.1	1416	10
1430	14	-	210	30.1	40.9	32.1		
1505	14	-	200	30.5	40.7	33.2	1518	9
1539	16	-	195	31.4	39.3	34.6		
1603	16	-	191	30.6	37.5	36.3	1617	9
1632	13	-	189	30.2	36.2	30.2		
1700	10	-	150	29.5	33.9	39.3	1716	9
1730	10	-	116	27.7	32.2	40.3		
1800	9	-	108	27.0	29.5	43.4		

(continued)

*Instantaneous readings of a Dasibi ozone monitor.
†Dash indicates below detection limit: HNO_3, 6 ppb; NH_3, 4 ppb; HCHO, 6 ppb.

TABLE A-15 (continued)

TIME (PDT)	HNO_3	NH_3	O_3 (ppb)	T(°C) AMBIENT	T(°C) CELL	% RH CELL	TIME (PDT)	HCHO
				AUGUST 27 (continued)				
1900	6	-	70	23.5	24.7	53.3		
1922	6	-	51	22.4	23.3	57.2		
1944	-	-	45	21.7	22.4	60.8		
2003	-	-	40	21.4	21.7	63.4		
2020	-	-	25	21.2	21.6	63.5		
2042	-	-	19	20.6	20.8	60.3		
2101	-	-	12	20.3	20.3	71.0		
2120	-	-	10	19.9	20.1	73.3		
2144	-	-	3	19.4	19.9	75.5		
2202	-	-	1	19.2	19.7	77.1		
2221	-	-	0	19.0	19.6	78.9		
2243	-	-	0	18.8	19.3	82.0		
2300	-	-	0	18.5	19.2	85.6		
2323	-	-	0	18.3	18.9	80.1		
2342	-	-	0	18.0	18.3	91.1		
				AUGUST 28 (TUESDAY)				
0000	-	-	0	18.2	18.5	92.2		
							0017	-
0033	-	-	0	17.7	18.4	94.2		
0100	-	-	0	17.8	18.5	95.6		
							0015	-
0130	-	-	0	17.8	18.8	97.0		
							0217	6
0235	-	-	0	17.3	18.5	98.1		
0305	-	-	0	17.3	18.1	98.9		
							0325	6
0337	-	-	0	17.2	18.2	99.8		
0400	-	-	0	17.3	18.4	99.9		
							0416	6
0430	-	-	11	17.3	18.2	99.1		
0500	-	-	10	17.3	18.7	99.8		
							0516	-
0530	-	-	12	17.4	18.7	100		
0600	-	-	15	17.4	18.7	99.0		
							0618	-
0633	-	-	17	17.7	18.9	99.6		
							0648	-
0708	-	-	10	17.8	19.2	98.1		

(continued)

TABLE A-15 (continued)

TIME (PDT)	HNO_3	NH_3	O_3 (ppb)	T(°C) AMBIENT	T(°C) CELL	% RH CELL	TIME (PDT)	HCHO
				AUGUST 28 (continued)				
							0730	-
0743	-	-	8	18.3	19.2	96.3		
0800	-	-	19	18.3	20.2	94.8		
							0815	7
0840	-	-	12	18.2	19.4	91.4		
0900	-	-	20	19.2	21.6	88.1		
							0930	-
0947	-	-	27	20.4	23.4	82.1		
1007	-	-	42	20.4	23.5	82.3		
							1020	6
1035	-	-	47	19.3	25.4	72.9		
1102	-	-	41	19.8	24.8	72.4		
							1117	6
1136	-	-	40	20.0	25.4	71.1		
1202	-	-	53	21.0	26.6	60.6		
							1218	6
1232	6	-	55	20.0	25.9	68.0		
1300	6	-	54	20.6	28.4	64.0		
							1316	11
1331	6	-	67	21.4	29.3	61.9		
1400	8	-	78	23.5	31.6	50.0		
							1415	10
1432	9	-	77	22.8	32.7	53.9		
1502	10	-	89	23.1	31.4	53.9		
							1518	9
1530	10	-	92	24.9	31.5	53.0		
1600	10	-	96	23.2	30.2	53.4		
							1617	15
1633	10	-	101	23.2	29.7	53.6		
1701	8	-	87	23.6	28.9	53.3		
1732	6	-	77	23.1	27.4	55.0		
1803	6	-	76	22.6	24.8	58.1		
				AUGUST 29 (WEDNESDAY)				
0645	-	-	3	17.5	19.8	79.1		
0704	-	-	2	17.8	19.4	80.3		
0718	-	-	0	17.9	19.5	80.0		
0730	-	-	0	17.8	19.3	80.1		
0745	-	-	0	18.1	19.5	80.1		
0800	-	-	7	18.2	19.8	79.1		

(continued)

TABLE A-15 (continued)

TIME (PDT)	HNO_3	NH_3	O_3 (ppb)	T(°C) AMBIENT	T(°C) CELL	% RH CELL	TIME (PDT)	HCHO
				AUGUST 29 (continued)				
0800	-	-	7	18.2	19.8	79.1		
0816	-	-	31	19.1	19.9	77.9		
0830	-	-	29	19.2	20.3	77.4		
0845	-	-	9	18.7	20.9	76.2		
0903	-	-	15	18.7	21.4	74.1		
							0916	-
0930	-	-	23	20.2	22.4	70.5		
1001	-	-	33	20.0	22.8	67.5		
							1016	-
1037	-	-	32	20.5	23.0	63.1		
1104	-	-	38	20.7	30.1	50.6		
							1120	-
1140	6	-	41	22.9	30.2	56.0		
1200	6	-	49	23.9	30.9	53.3		
							1215	8
1230	9	-	50	22.2	30.2	53.8		
1300	9	-	58	22.5	31.2	49.6		
							1315	10
1330	8	-	61	25.9	33.6	48.5		
1401	7	-	66	25.4	35.6	44.1		
1438	8	-	74	23.8	31.3	47.5		
1503	8	-	62	24.5	32.7	47.5		
1516	6	-	61	23.2	32.7	47.0		
1534	6	-	63	23.6	31.2	48.4		
1548	6	-	64	22.9	30.4	48.9		
1603	6	-	63	24.2	30.1	49.5		
1618	-	-	67	22.8	29.8	49.9		
1636	-	-	73	23.3	28.9	51.2		
1650	-	-	73	24.0	29.0	51.1		
1715	-	-	77	22.8	27.1	54.1		
1730	-	-	74	22.1	26.1	55.2		
1745	-	-	61	21.5	24.2	50.1		
1800	-	-	57	21.1	23.3	60.3		
				AUGUST 30 (THURSDAY)				
0855	6	-	9	19.6	25.6	69.0		
							0925	≤ 7
0940	8	NP	25	21.0	27.6	63.5		
1002	6	NP	32	21.7	28.3	58.4		

NP = No plot - unretrievable data.

(continued)

TABLE A-15 (continued)

TIME (PDT)	HNO_3	NH_3	O_3 (ppb)	T(°C) AMBIENT	T(°C) CELL	% RH CELL	TIME (PDT)	HCHO
				AUGUST 30 (continued)				
							1020	≤10
1033	7	-	41	21.6	29.0	57.0		
1100	8	-	49	23.1	31.2	54.1		
							1115	≤12
1130	9	-	55	23.3	34.6	49.9		
1200	-	-	70	24.4	38.5	42.3		
							1218	≤10
1235	11	-	78	24.3	38.0	41.0		
1305	10	-	81	26.2	37.0	40.6		
							1321	≤12
1335	13	NP	104	25.5	38.1	38.3		
1410	12	-	113	26.2	38.6	36.9		
1430	8	-	120	28.5	38.9	35.9		
1445	12	-	138	25.4	37.7	36.6		
1503	10	NP	133	27.1	37.1	37.2		
1515	9	NP	130	27.0	36.4	37.2		
1530	9	NP	134	26.5	35.7	38.3		
1545	9	NP	140	27.4	34.9	38.8		
1600	12	NP	158	26.5	33.3	41.6		
1618	8	NP	164	26.5	33.3	41.6		
1637	6	NP	151	26.5	31.1	45.6		
1648	11	NP	139	26.3	31.8	45.6		
1708	7	NP	128	25.6	30.8	46.5		
1719	6	NP	115	24.6	29.6	48.3		
1732	-	NP	94	24.0	28.0	50.5		
1746	7	NP	89	23.4	26.9	51.9		
1800	7	NP	79	23.2	25.7	54.8		
				AUGUST 31 (FRIDAY)				
0835	7	-	33	19.0	30.9	61.0		
0908	-	-	28	20.3	30.7	58.9		
0920	7	-	34	20.3	31.0	57.5		
0931	7	-	40	20.6	30.9	57.1		
0945	8	-	48	21.7	32.2	56.4		
1000	6	-	55	22.4	32.7	54.1		
1015	9	-	64	22.6	34.1	52.4		
1038	10	4	95	23.1	34.2	49.3		
1049	10	5	91	23.8	35.4	47.5		
1107	12	NP	92	24.6	37.0	45.3		
1120	12	6	97	25.6	38.2	42.3		

TABLE A-15 (continued)

TIME (PDT)	HNO_3	NH_3	O_3 (ppb)	T(°C) AMBIENT	T(°C) CELL	% RH CELL	TIME (PDT)	HCHO
				AUGUST 31 (continued)				
1137	14	6	107	26.4	37.8	41.2		
1151	11	6	113	26.5	38.6	39.4		
1206	15	7	124	27.0	39.3	38.4		
1227	15	-	140	28.3	38.4	37.1		
1247	15	-	131	27.6	39.5	36.4		
1303	13	-	122	27.3	39.6	36.1		
							1320	≤6
1339	15	-	163	26.9	38.6	37.0		
1400	12	-	166	27.1	38.4	38.2		
							1415	≤8
1430	15	-	179	26.8	37.6	37.1		
1445	16	-	[illegible]5	27.9	37.5	37.1		
1500	13	-	192	27.0	37.4	37.5		
							1515	≤11
1530	14	-	176	28.2	36.5	39.4		
1545	13	-	167	28.0	35.9	40.1		
1603	13	-	154	28.2	33.6	43.0		
							1616	≤6
1639	10	-	113	26.7	32.8	44.8		
1702	9	-	125	26.0	31.8	44.4		
							1715	≤11
1731	9	-	136	26.0	29.7	47.5		
1745	7	-	130	25.6	28.7	48.9		
1800	6	-	129	24.7	27.2	52.2		
							1820	≤6
1842	-	-	92	22.9	23.8	59.8		
				SEPTEMBER 1 (SATURDAY)				
0600	-	-	1	16.8	18.5	89.6		
							0623	-
0637	-	-	5	17.3	18.5	89.3		
0703	-	-	8	18.0	18.5	87.8		
							0723	7
0737	-	-	12	18.7	20.1	86.3		
0803	-	-	11	18.2	19.8	85.4		
							0828	9
0847	-	-	16	19.9	21.6	88.4		
0907	-	-	25	19.9	23.7	78.2		
							0920	13
0935	6	-	25	20.2	23.9	75.1		

(continued)

TABLE A-15 (continued)

TIME (PDT)	HNO_3	NH_3	O_3 (ppb)	T(°C) AMBIENT	T(°C) CELL	% RH CELL	TIME (PDT)	HCHO
				SEPTEMBER 1 (continued)				
1000	7	6	33	20.8	30.5	67.0		
							1020	12
1039	8	8	45	22.1	32.1	50.1		
1105	12	9	70	21.6	35.8	51.6		
							1121	12
1138	13	12	87	24.3	37.2	48.5		
							1200	9
1241	13	10	102	24.9	35.3	44.8		
1404	12	-	190	25.8	37.3	39.0		
1423	14	4	181	27.8	37.2	39.1		
1441	10	4	175	26.6	38.2	36.5		
1500	10	4	157	27.5	37.5	34.1		
1519	11	4	155	27.4	36.8	34.2		
1538	10	4	151	28.7	35.7	33.2		
1614	9	-	159	28.1	35.6	32.8		
1628	9	-	190	28.2	35.5	33.0		
1643	12	-	210	27.4	34.6	35.6		
1704	8	-	218	27.5	33.8	37.3		
1718	11	-	222	27.4	32.5	38.0		
1731	14	-	230	27.5	31.6	40.8		
1748	9	-	225	26.1	29.8	43.2		
1822	9	-	190	24.8	26.3	49.3		
1837	-	-	161	23.9	24.8	52.1		
1852	-	-	127	23.2	23.8	54.5		
1907	-	-	104	22.4	22.7	57.0		
1922	6	-	81	22.0	21.8	59.3		
2055	-	-	6	18.7	18.2	72.8		
2125	-	-	0	17.9	17.2	70.2		
				SEPTEMBER 2 (SUNDAY)				
1015	7	6	100	25.3	33.9	36.8		
1030	10	6	128	25.4	38.6	36.4		
1048	10	7	140	25.5	38.7	35.1		
1105	11	5	141	27.4	40.1	33.8		
1138	13	4	160	27.6	38.7	33.8		
1202	12	-	162	27.4	38.9	31.8		
1222	13	-	160	27.7	39.8	30.0		
1238	13	-	164	30.0	40.6	27.1		
1255	11	-	164	30.3	41.1	27.3		

(continued)

TABLE A-15 (continued)

TIME (PDT)	HNO_3	NH_3	O_3 (ppb)	T(°C) AMBIENT	T(°C) CELL	% RH CELL	TIME (PDT)	HCHO
				SEPTEMBER 2 (continued)				
							1310	20
1340	10	-	174	31.3	41.9	23.3		
1400	9	-	160	30.7	40.8	23.1		
1417	9	-	160	31.2	41.3	22.8		
1431	9	-	175	31.6	41.7	22.2		
1445	9	-	190	30.6	40.3	21.8		
1500	8	-	185	30.3	39.2	24.1		
							1515	21
1530	9	-	214	31.0	38.5	25.2		
1547	9	-	220	30.3	37.8	27.2		
1602	8	-	210	30.0	37.1	28.1		
1616	9	-	230	29.5	36.6	32.0		
1633	8	-	198	30.2	35.8	33.1		
1649	7	-	165	29.1	35.2	31.9		
1703	7	-	170	28.7	34.5	33.3		
							1718	19
1731	6	-	152	28.1	32.0	35.2		
1755	6	-	107	27.5	30.1	36.5		
1815	-	-	99	26.7	28.4	39.3		
1830	-	-	86	25.9	27.1	42.3		
1845	-	-	82	25.5	26.1	44.3		
1900	-	-	73	24.5	25.2	46.4		
							1915	20
1931	-	-	61	23.8	23.7	50.8		
2125	-	-	4	20.7	20.0	62.5		
2250	-	-	0	20.2	19.2	67.0		
				SEPTEMBER 3 (MONDAY)				
1015	9	-	112	26.6	38.1	36.5		
1030	18	4	142	27.3	40.7	33.2		
1046	20	4	138	27.4	40.9	32.0		
1102	15	5	150	28.9	41.6	31.4		
1116	11	-	170	28.7	41.2	30.1		
1137	10	4	166	29.7	42.0	28.4		
1151	10	-	120	30.3	43.0	26.9		
1207	11	-	159	29.9	43.0	26.9		
1220	13	-	171	30.0	41.4	27.1		
1235	13	-	183	30.9	43.5	26.3		
1251	14	4	201	31.2	43.0	26.1		
1305	13	-	191	32.1	42.9	26.3		
1318	14	4	200	31.0	42.7	26.5		

(continued)

TABLE A-15 (continued)

TIME (PDT)	HNO_3	NH_3	O_3 (ppb)	T(°C) AMBIENT	T(°C) CELL	% RH CELL	TIME (PDT)	HCHO
				SEPTEMBER 3 (continued)				
1347	15	-	200	32.9	43.2	25.6		
1402	15	-	219	32.2	43.3	24.8		
1417	15	-	239	32.0	42.2	24.1		
1430	16	-	253	31.0	40.6	25.9		
1448	18	-	259	33.5	40.4	26.0		
1504	17	-	252	32.6	42.1	24.5		
1519	19	-	267	32.8	41.1	24.9		
1532	19	-	266	33.6	40.5	26.1		
1547	18	-	307	32.0	39.7	29.3		
1602	22	-	287	32.8	38.8	30.1		
1617	21	-	255	31.5	38.2	31.6		
1632	20	-	210	31.5	37.7	32.3		
1646	17	-	180	31.3	37.1	32.1		
1704	15	-	152	30.8	36.6	32.1		

TABLE A-16. HOURLY AVERAGE CONCENTRATIONS (PPB) OF PAN BY GC MEASUREMENT*

TIME (PDT)	8/27	8/28	8/29	8/30	8/31	9/1	9/2	9/3
0000-0100		0	0	0	2	2	4	3
0100-0200		0	0	0	2	1	4	3
0200-0300		1	0	0	3	1	4	4
0300-0400		1	1	0	3	1	4	4
0400-0500		1	1	0	3	1	4	5
0500-0600		1	1	0	3	2	4	5
0600-0700	5	1	0	0	3	2	2	4
0700-0800	4	1	0	0	3	2	3	4
0800-0900	3	1	1	1	2	2	4	5
0900-1000	4	1	1	0	2	2	5	4
1000-1100	5	2	1	1	3	2	7	4
1100-1200	7	2	1	1	4	4	7	4
1200-1300	8	3	2	2	5	4	7	5
1300-1400	8	3	2	3	5	7	5	7
1400-1500	7	3	2	4	7	10	5	10
1500-1600	8	4	2	5	7	7	7	11
1600-1700	3	4	2	7	5	8	10	10
1700-1800	2	3	3	4	5	11	5	3
1800-1900	1	2	3	2	4	10	3	2
1900-2000	1	1	2	2	3	4	2	1
2000-2100	1	0	1	2	2	2	1	1
2100-2200	1	0	1	1	1	1	2	
2200-2300	0	0	1	1	1	2	4	
2300-2400	0	0	0	0	1	3	2	

*Verified by long-path FT-IR results for several points in the 3-11 ppb range.